Supporting Information

Chiral Benzothiazole Monofluoroborate Featuring Chiroptical and Oxygen Sensitizing Properties: Synthesis and Photophysical Studies.

Omar Sadek,[a,b] Laura Abad Galán,[c] Frédéric Gendron,[d] Bruno Baguenard,[e] Stephan Guy,[e] Amina Bensalah-Ledoux,[e] Boris Le Guennic,*[d] Olivier Maury,*[c] David M. Perrin,[b] Emmanuel Gras*[a,f]‡

(a) LCC, CNRS UPR 8241, Université de Toulouse, UPS, INPT, 205 route de Narbonne 31077 Toulouse Cedex 4

(b) Department of Chemistry, 2036 Main Mall, UBC, Vancouver, BC, V6T 1Z1, Canada

(c) Univ. Lyon, ENS de Lyon, CNRS UMR 5182, Laboratoire de Chimie, F-69342 Lyon, France.

(d) Univ Rennes, CNRS, ISCR (Institut des Sciences Chimiques de Rennes) - UMR 6226, F-35000 Rennes (France)

(e) Univ. Lyon, Institut Lumière Matière, UMR 5306 CNRS–Université Claude Bernard Lyon 1, 10 rue Ada Byron, 69622 Villeurbanne Cedex, France.

(f) ITAV, CNRS USR 3505, Université de Toulouse, UPS, 1 place Pierre Potier, 31106 Toulouse Cedex 1.

‡ New address: Laboratoire Hétérochimie Fondamentale et Appliquée, Université Paul Sabatier/CNRS UMR 5069, 118 Route de Narbonne, 31062 Toulouse Cedex 09, France

Table of Contents

General Information

Spectroscopic Details

Absorption spectra were recorded on a JASCO V-650 spectrophotometer in diluted solution (ca. 10^{-5} or 10^{-6} mol L^{-1}), using spectrophotometric grade solvents. Emission spectra were measured using Horiba-Jobin-Yvon Fluorolog-3 fluorimeter. The steady-state luminescence was excited by unpolarised light from a 450 W xenon continuous wave (CW) lamp and detected at an angle of 90° for measurements of dilute solutions (10 mm quartz cuvette) by using a Hamamatsu R928. Spectra were corrected for both excitation source light-intensity variation and emission spectral responses. Luminescence quantum yields Q were measured in diluted solutions with an absorbance lower than 0.1, by using the following Equation 1:

$$\frac{Qx}{Qr} = \left[\frac{Ar(\lambda)}{Ax(\lambda)}\right] \cdot \left[\frac{n_x^2}{n_r^2}\right] \cdot \left[\frac{Dx}{Dr}\right] \qquad (1)$$

where A(λ) is the absorbance (or optical density) at the excitation wavelength, n the refractive index of the solvent and D the integrated luminescence intensity. “r” and “x” stand for reference and sample, respectively. Here, the reference is coumarin-153 in methanol (Qr = 0.45). Excitations of reference and sample compounds were performed at the same wavelength. The reported results are the average of 4‑5 independent measurements at various absorbances (comprised between 0.01‑0.1) for both sample and reference. The plot of the integrated luminescence intensity vs. absorbance gives straight line with excellent correlation coefficients and the slope S can be determined for both sample (x) and reference (r). Equation 1 becomes Equation 2.

$$\frac{Qx}{Qr} = \left[\frac{Sx}{Sr}\right] \cdot \left[\frac{n_x^2}{n_r^2}\right] \qquad (2)$$

For singlet oxygen quantum yield determination φ_Δ, the principle is exactly the same except that the singlet oxygen luminescence emission band (D) is integrated for both sample (x) and reference (r) compounds. A(λ) is the absorbance (or optical density) at the excitation wavelength. In this case it is very important that both experiments are

conducted in the same solvent at exactly the same excitation wavelength (nx = nr). The reported results are the average of 4–5 independent measurements at various absorbances (comprised between 0.01–0.1) for both sample and reference. The plot of the integrated singlet oxygen luminescence intensity vs. absorbance gives straight line with excellent correlation coefficients and the slope S can be determined for both sample (x) and reference (r). In the present case, the reference is phenalenone ($\varphi_{\Delta r}$ = 0.98 in dichloromethane).

ECD spectra were recorded on a homemade CD spectrometer, at room temperature, and using a 1 cm path length quartz cells. We used the standard setup: Xenon lamp, Rochon polarizer, photoelastic modulator with lockin (1f) and DC detection. Spectra were measured in the 220-450 nm wavelength range with a 1 nm increment and a 2 s integration time. Spectra were baseline-corrected.

CPL spectra were recorded on an in-house-developed apparatus. Unpolarized light coming from a 288 nm LED is focused on 1x1 cm² quartz cell. Fluorescence light emitted by the sample is collected at 45 °. F2 is a long pass filter (λ > 300 nm). The photo-elastic modulator (PEM, 50 kHz) associated with the polarizer at 45 ° allows to record both the luminescence and the CPL signals by combining the DC and 1f signal from the PMT. Spectra are recorded with a step of 1nm and an integration time of 7s and are further processed by applying a Savitzky Golay filter.

Computational Details

Kohn-Sham Density Functional Theory Calculations. The 2017's release of the Amsterdam Density Functional (ADF[1,2,3]) software package was used to perform structural optimizations of the **1s** complex. The ground state (GS) geometries were obtained using Kohn-Sham density functional theory (DFT), whereas the structures of the excited states (ES) were obtained by using the time-dependent DFT (TD-DFT).[4] These calculations utilized the scalar all-electron zeroth-order regular approximation (ZORA[5]) along with several functionals: the hybrid functional B3LYP[6,7] (Becke, 3-parameters Lee-Yang-Parr) with 20% of exact exchange, and the hybrid functional PBE0[8,9] with 25% of

exact exchange and CAM-B3LYP[10] (range-separated exchange with eX varying from 19 to 65% with increasing inter electronic distance). The atomic basis set corresponded to the triple-ζ polarized Slater-type orbital (STO) all-electron basis set with two sets of polarization functions for all atoms (TZ2P[11]).

The absorption and emission properties, i.e. oscillator strengths and rotatory strengths were obtained within the Excitations module implemented in ADF.[12,13] Solvent effects were taken into account by using the Conductor-Like Screening Model (COSMO) with the dielectric constant of 8.9 to model dichloromethane.[14] The rotatory strengths were calculated using the dipole-velocity representation.[15] The nature of the transitions involved in the CD and CPL spectra was analyzed with the help of the Natural Transition Orbitals (NTOs).[16] The NTOs were then visualized with the graphical user interface of ADF.

Multi-Reference Calculations. The wavefunction calculations were performed using the Molcas 8.2 software package.[17] In these calculations, the complete active space self-consistent field[18] (CASSCF) approach and the complete active space perturbation theory at the second order[19] (CASPT2) were used to treat the static and dynamic correlation effects, respectively. The CASPT2 calculations were performed using the multi-state approach with an imaginary shift of 0.2 in order to avoid intruder states in the wavefunction. The second-order Douglas-Kroll-Hess[20,21,22,23] scalar relativistic Hamiltonian was used to treat the scalar relativistic effects in combination with the all-electron atomic natural orbital relativistically contracted (ANO-RCC) basis set from the Molcas library.[24,25,26] The basis sets were contracted to the triple-ζ plus polarization (TZP) quality (S = 17s12p5d4f2g/5s4p2d1f; B, C, N, O, F = 14s9p5d3f2g/4s3p2d1f; H = 8s4p3d1f/2s1p). The choice of the active space, namely CAS(10,10), was driven by the NTO analysis performed on this complex at the DFT level. The nature of the molecular orbital was analyzed then using natural orbitals (NOs) that were directly obtained from the multi-configurational wavefunctions that include SOC effects. The procedure to obtain these orbitals is explained in the References [27], [28] and [29]. The orbitals were then visualized with the graphical interface of the ADF software package.

The calculations employed the state-averaged formalism at the SR level by taking into account 6 singlet and 6 triplet spin states. The spin-orbit coupling (SOC) was then introduced within a state interaction among the basis of calculated SR states using the restricted active space state interaction (RASSI) approach.[30] Herein the SOC matrix is diagonalized using either the calculated SR CASSCF or SR CASPT2 energies. Therefore, in the manuscript the scalar and spin-orbit coupling results will be denoted as SCF/PT2-SR and SCF/PT2-SO, respectively.

NMR Identification of the Fluoride abstraction from 1

Figure S1: Evolution of ^{19}F (a), ^{11}B (b) and ^{1}H (c) NMR spectra of 1 with TMS-OTf.

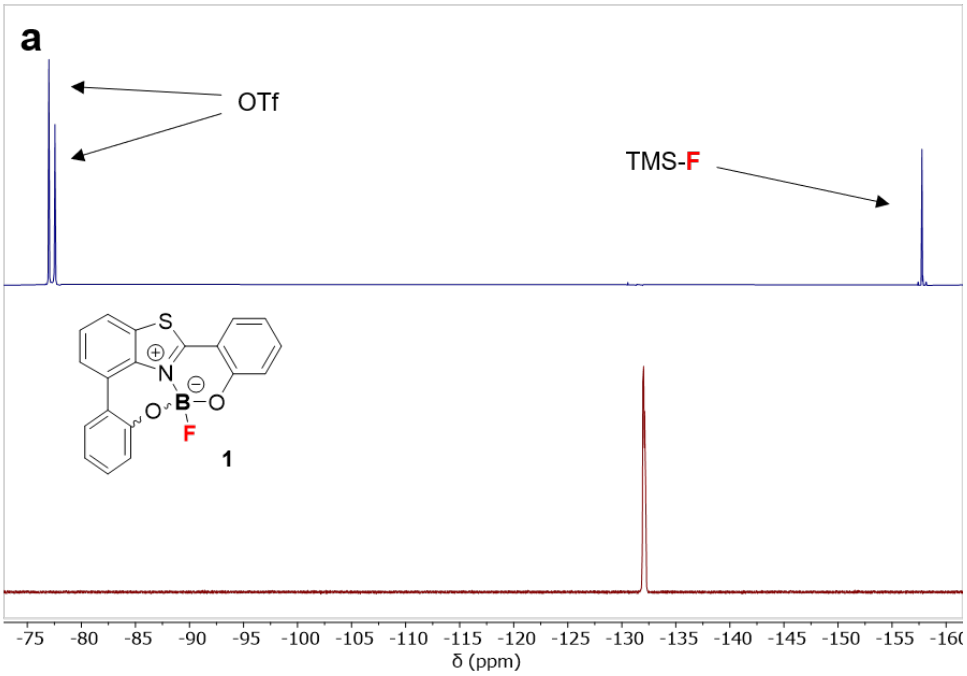

Figure S1a

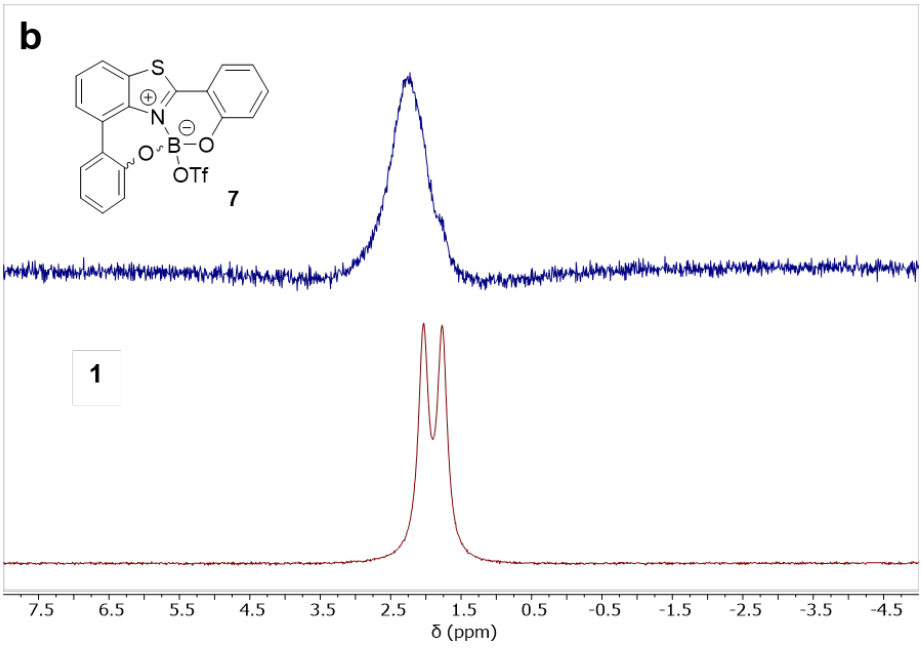

Figure S1b

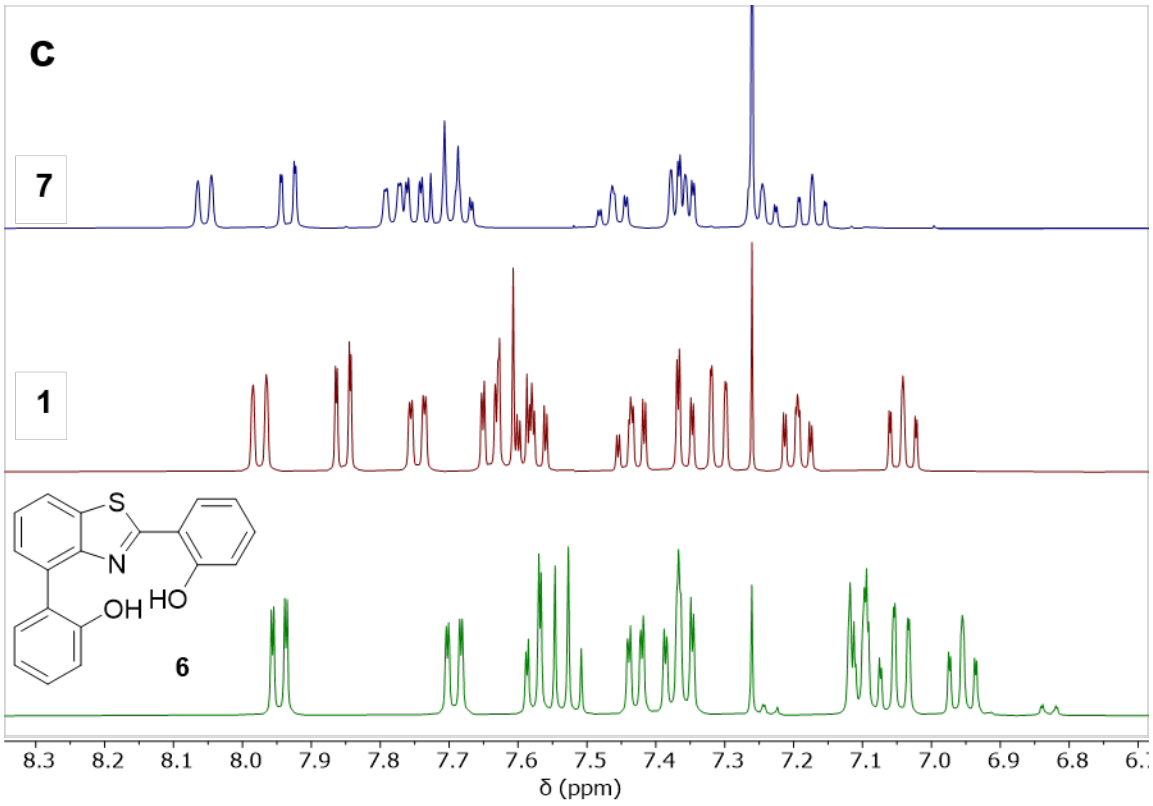

Figure S1c

Selected Structural Parameters of Complex 1 and Ligand 6

Table S1 Selected structural parameters from X-ray structure of complex 1.

	$\mathbf{1_R}$	$\mathbf{1_S}$
Selected Bond Lengths (Å)		
B-N	1.586(5)	1.589(5)
B-F	1.389(4)	1.392(4)
B-O_1	1.434(3)	1.450(4)
B-$O_{1'}$	1.427(4)	1.422(4)
Selected Plane, Torsion and Bond Angles (°)		
N-C_2-$C_{2'}$-$C_{1'}$	2.3(4)	-5.1(5)
Benzothiazole – Phenol O_1 planes	3.3	6.1
Benzothiazole – Phenol $O_{1'}$ planes	21.4	20.7
N-B-F	106.1(2)	106.6(2)
O_1-B-F	111.2(3)	110.7(3)
$O_{1'}$-B-F	113.1(3)	113.0(3)
O_1-B-O_1	108.6(3)	108.5(3)
N-B-O_1	109.3(2)	108.7(3)
N-B-$O_{1'}$	108.3(2)	109.3(3)
Tetrahedral Character at Boron	88%	89%

Table S2 Selected plane and torsion angles for ligand **6**

Plane or torsion	Angle (°)
Benzothiazole – Phenol O_1 planes	11.2
Benzothiazole – Phenol $O_{1'}$ planes	57.4
N-C_2-$C_{2'}$-$C_{1'}$ torsion	9.8(2)

HPLC Separation of Enantiomers of 1_{rac} and Stability of 1_A and 1_B

Figure S2a HPLC trace of $\mathbf{1}_{rac}$ (left), HPLC traces of enantiomers $\mathbf{1}_A$ (top right) and $\mathbf{1}_B$ (bottom right) after 1 week at room temperature in methanol.

Retention Time (min)	Area (%)
10.0 ($\mathbf{1}_A$)	50.1
14.4 ($\mathbf{1}_B$)	49.9

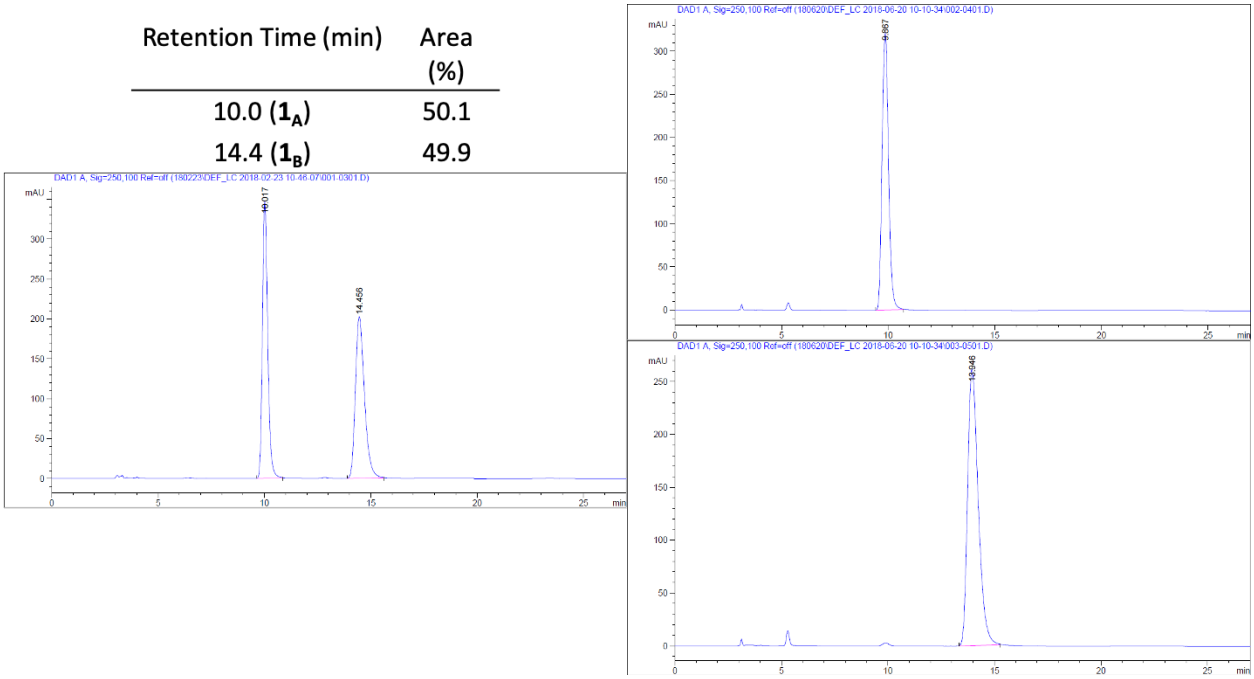

Figure S3b Evolution of the CD spectrum of 1B over 72h in MeCN/PBS (1:6) at room temperature.

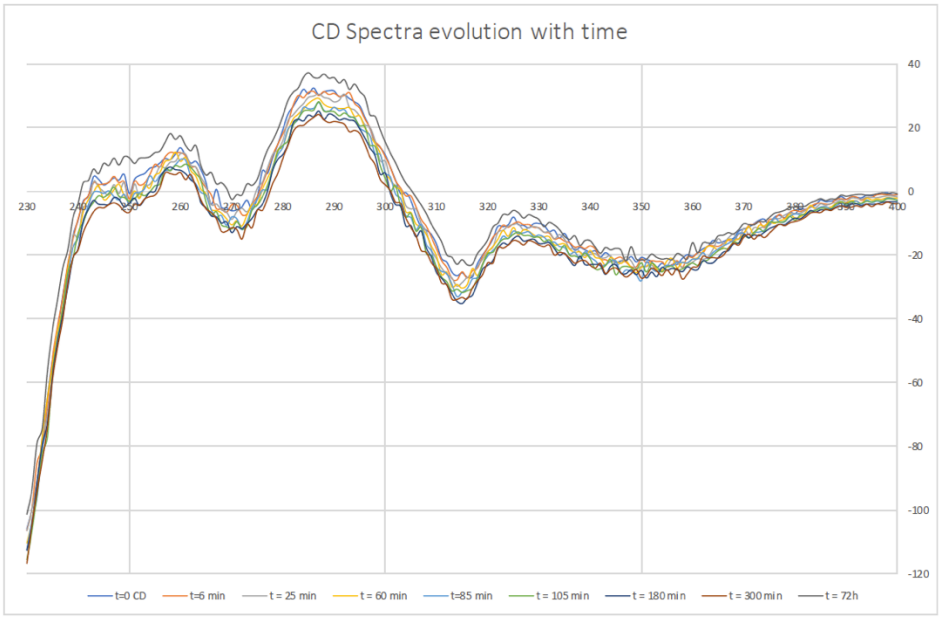

Comparison of NMR Spectra of Enantiomers 1_A and 1_B

Figure S4 Comparison of ^{1}H (top left), ^{19}F (top right) and ^{11}B (bottom) NMR spectra of $\mathbf{1_A}$ and $\mathbf{1_B}$.

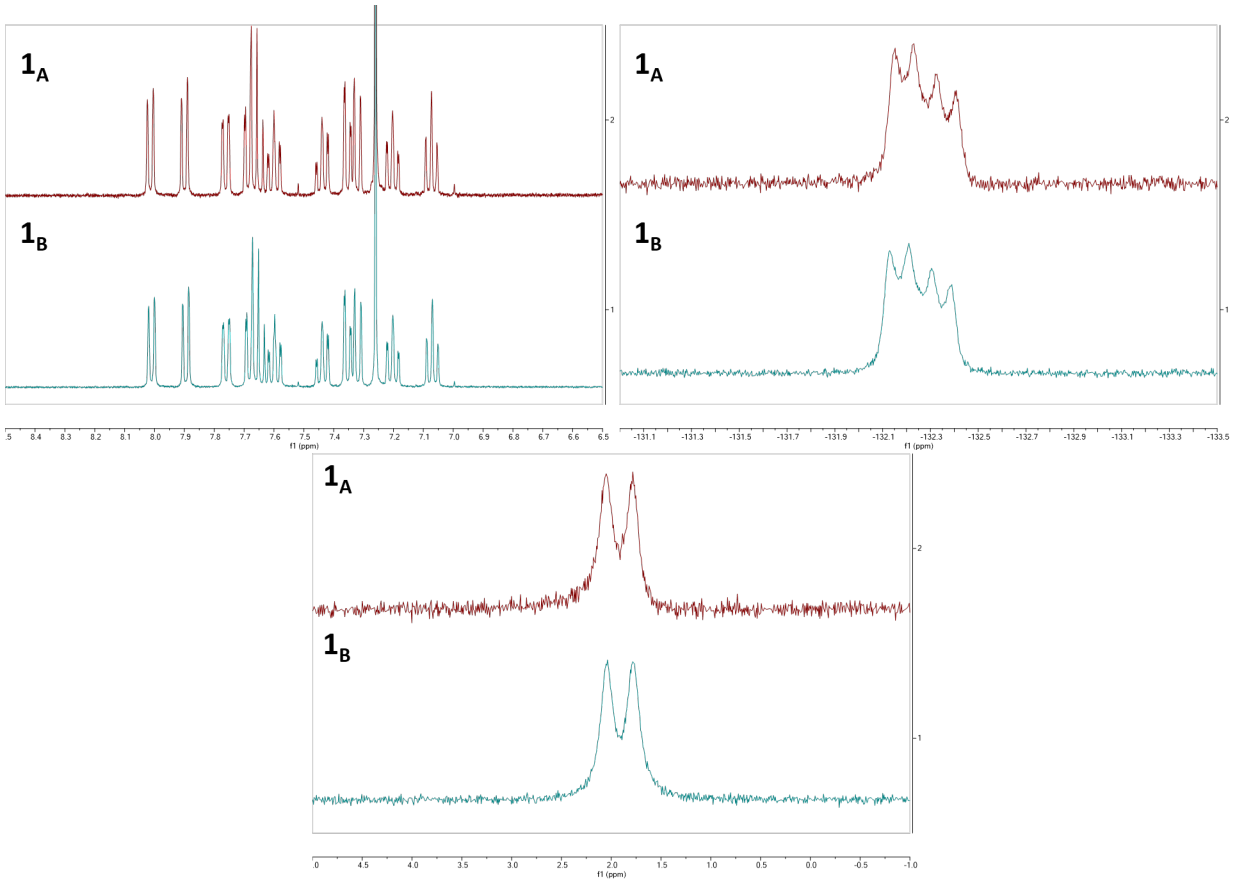

NMR Spectroscopic Stability Studies of Complex 1 in D_2O/CD_3CN (1:6)

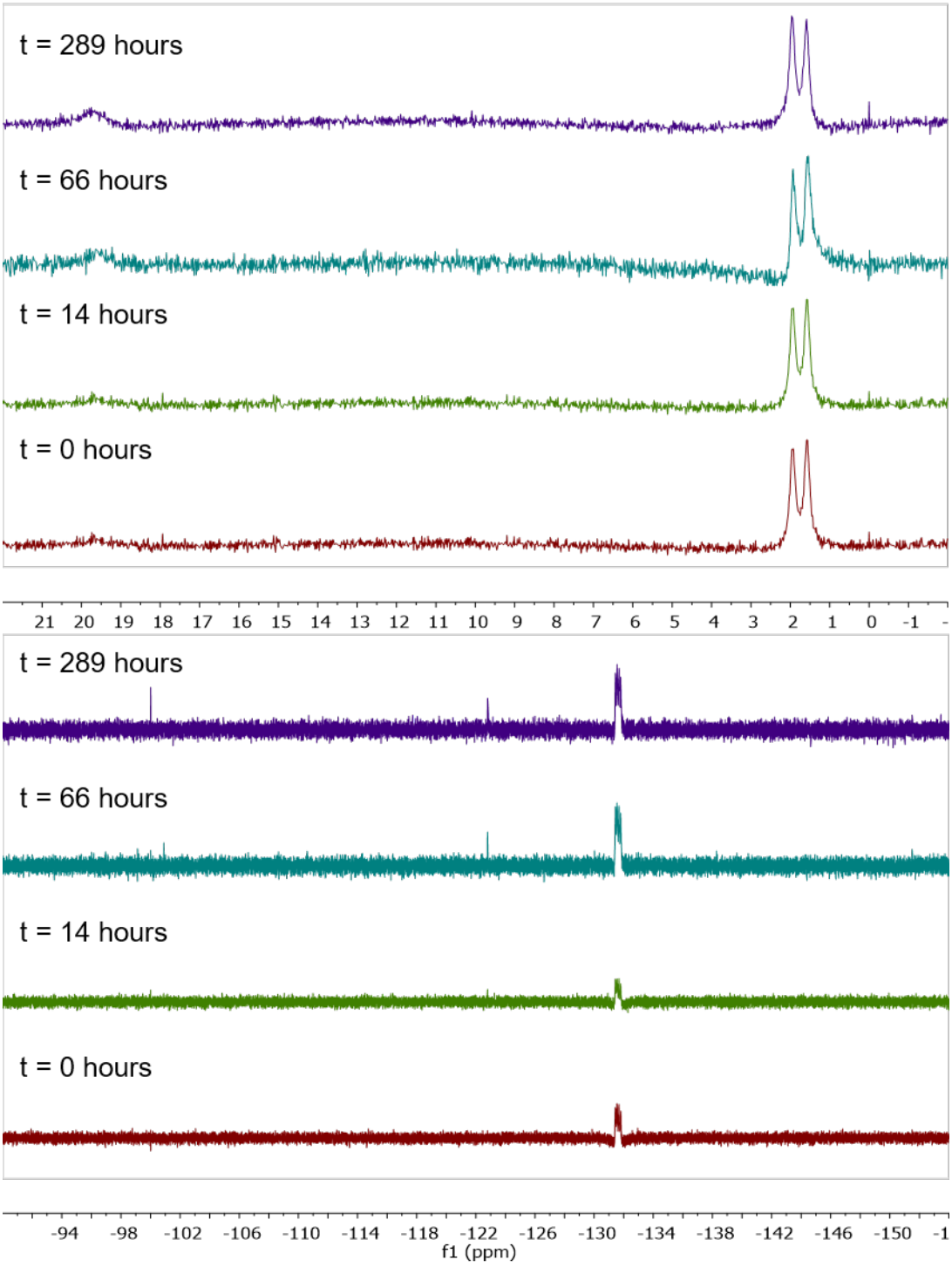

Figure S5 ^{11}B (top) and ^{19}F (bottom) NMR spectra evolution of **1** in CD_3CN/D_2O (1:6).

Photophysical Studies of Ligand 6 and Complex 1

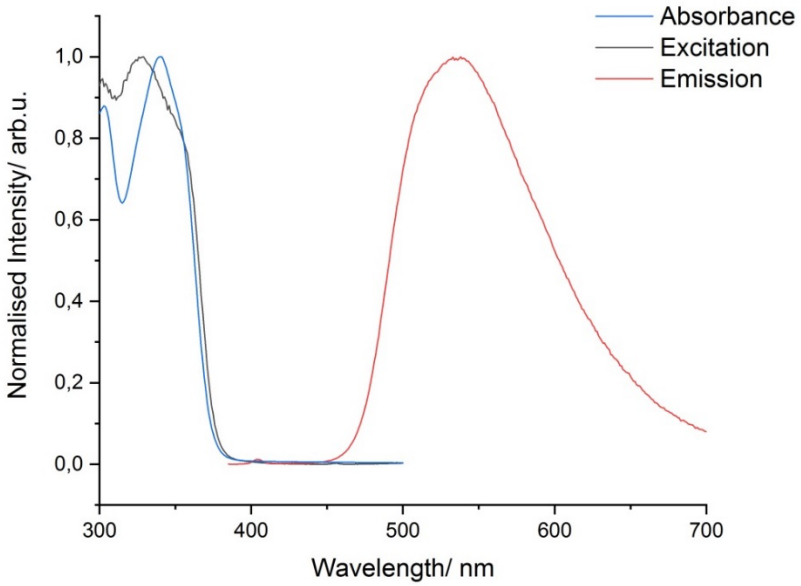

Figure S6 Normalised absorbance (blue), visible emission at λ_{exc}= 375 nm (red) and excitation at λ_{em}= 530 nm (black) for **6** in CH_2Cl_2 at room temperature.

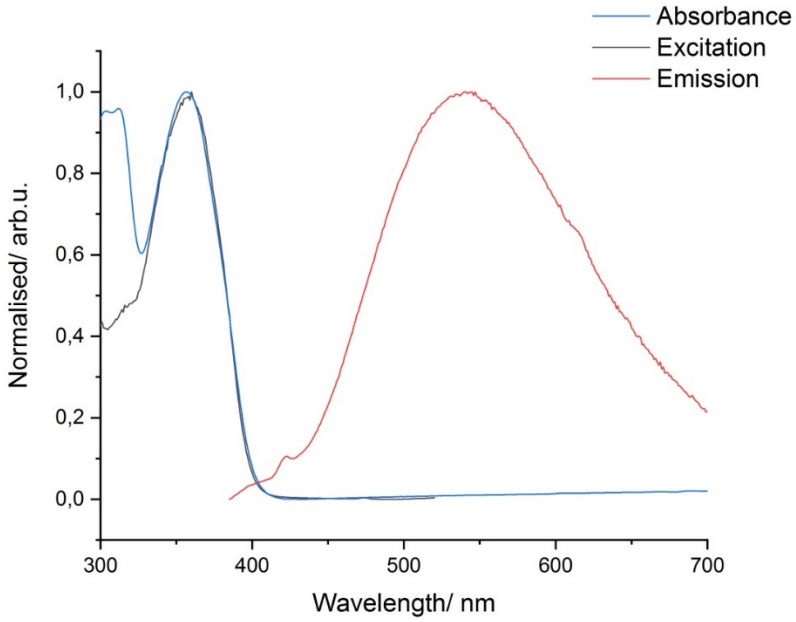

Figure S7 Normalised absorbance (blue), visible emission at λ_{exc}= 375 nm (red) and excitation at λ_{em}= 540 nm (black) for **1** in MeOH at room temperature.

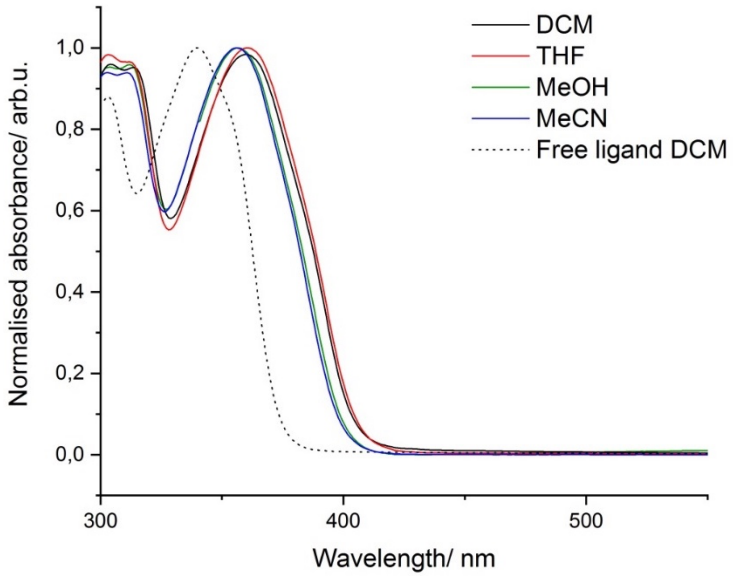

Figure S8 Normalised absorption of complex **1** (solid line) and ligand **6** (dotted line) in CH_2Cl_2 (black), THF (red), MeOH (green) and MeCN (blue) at room temperature.

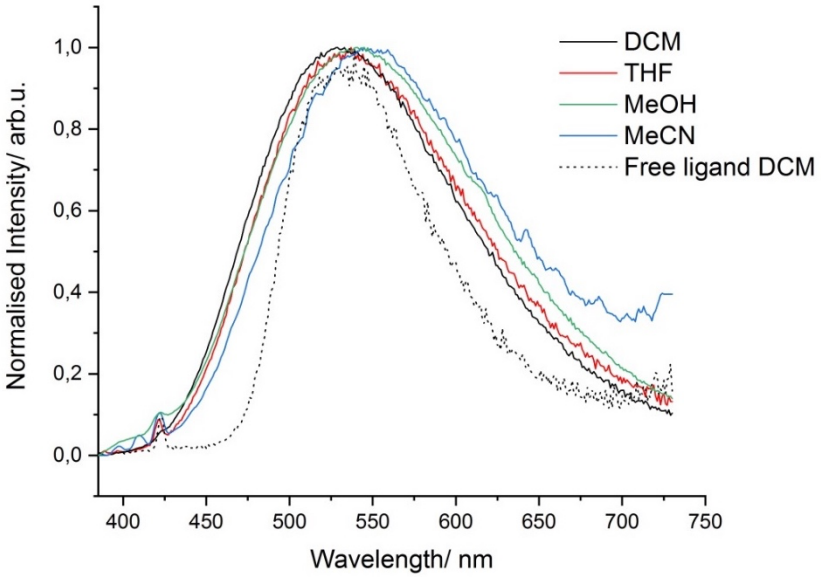

Figure S9 Normalised emission of complex 1 (solid line) and ligand **6** (dotted line) in CH_2Cl_2 (black), THF (red), MeOH (green) and MeCN (blue) at room temperature (λ_{exc}= 375 nm).

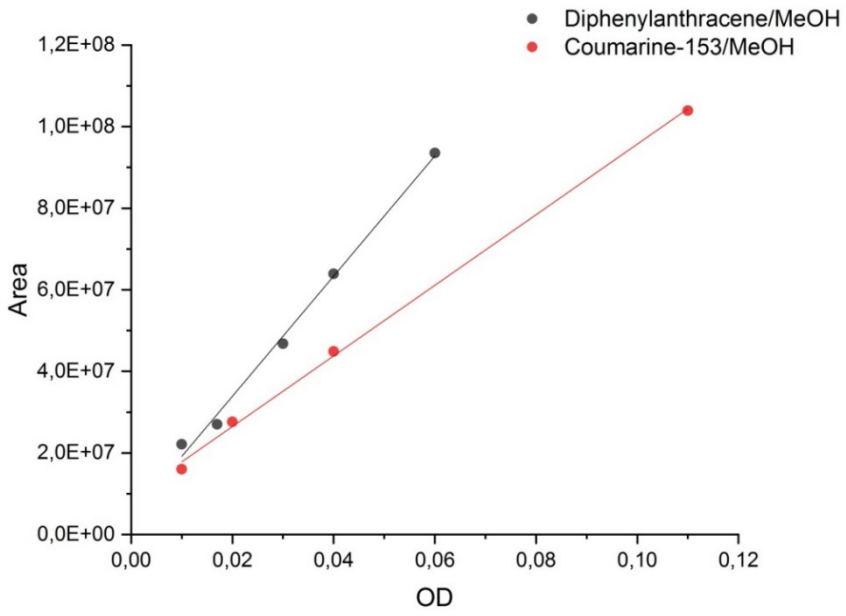

Figure S10 Integrated luminescence area according to optical density of the reference, diphenyl anthracene in MeOH (black) and Coumarine-153 in MeOH (red) to validate the method.

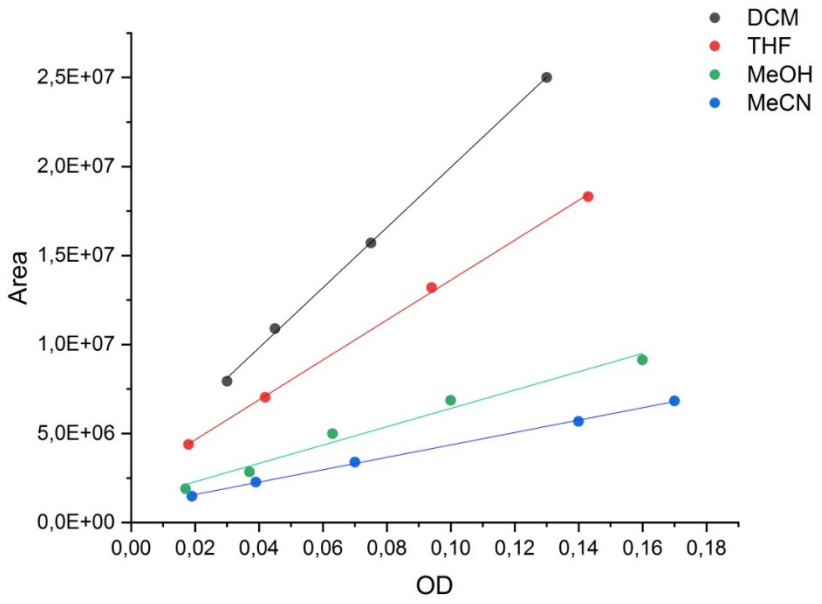

Figure S11 Integrated luminescence area according to optical density of **1** in CH_2Cl_2 (black), THF (red) MeOH (green) and MeCN (blue) at room temperature.

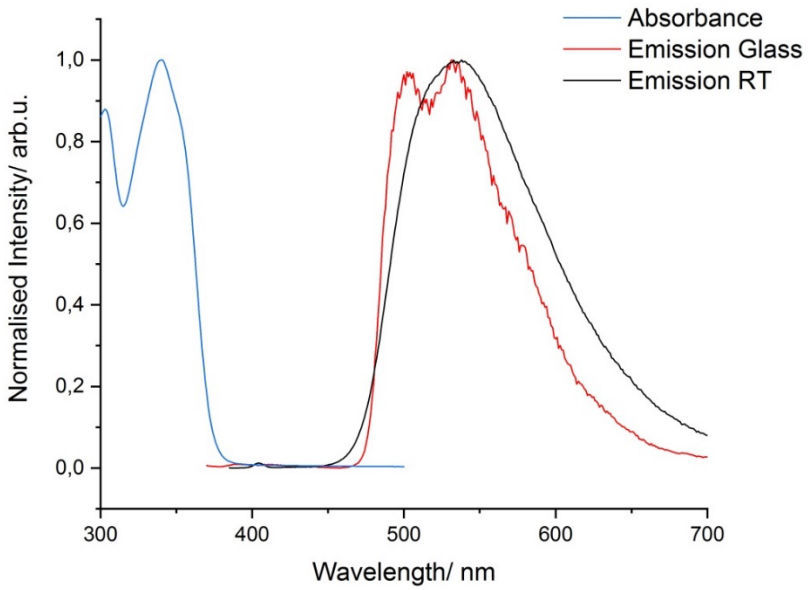

Figure S12 Absorbance (blue) and emission of **6** at room temperature in CH_2Cl_2 (black) and 77K in MeOH/EtOH (1:4) (red). After delay of 0.05 ms no emission is found at 77K (suggestive of singlet character).

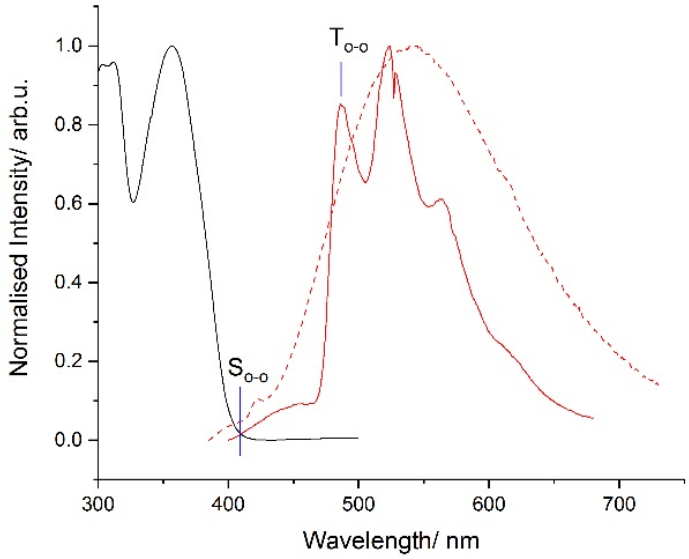

Figure S13 Absorbance (black) and emission (red trace) of **1** at room temperature in MeOH (dashed line) and 77K in MeOH/EtOH (1:4).

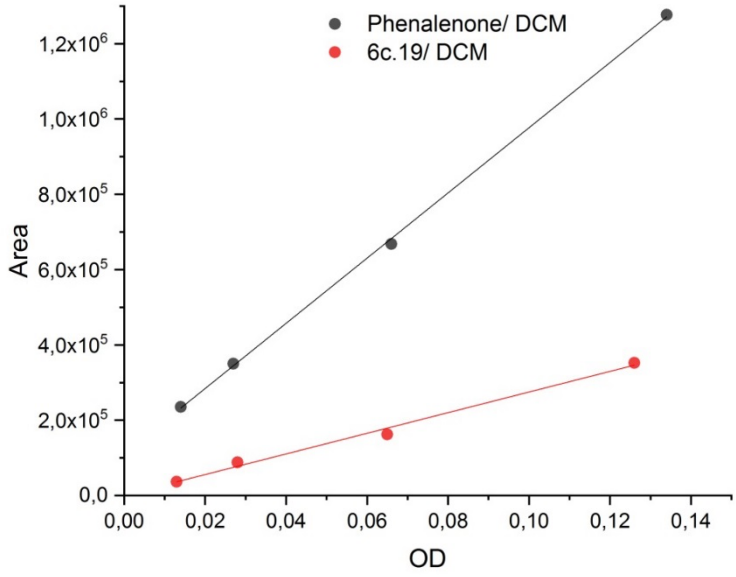

Figure S14 Integrated singlet oxygen emission area according to optical density of phenalenone (black) and **1** (red) in CH_2Cl_2 at room temperature.

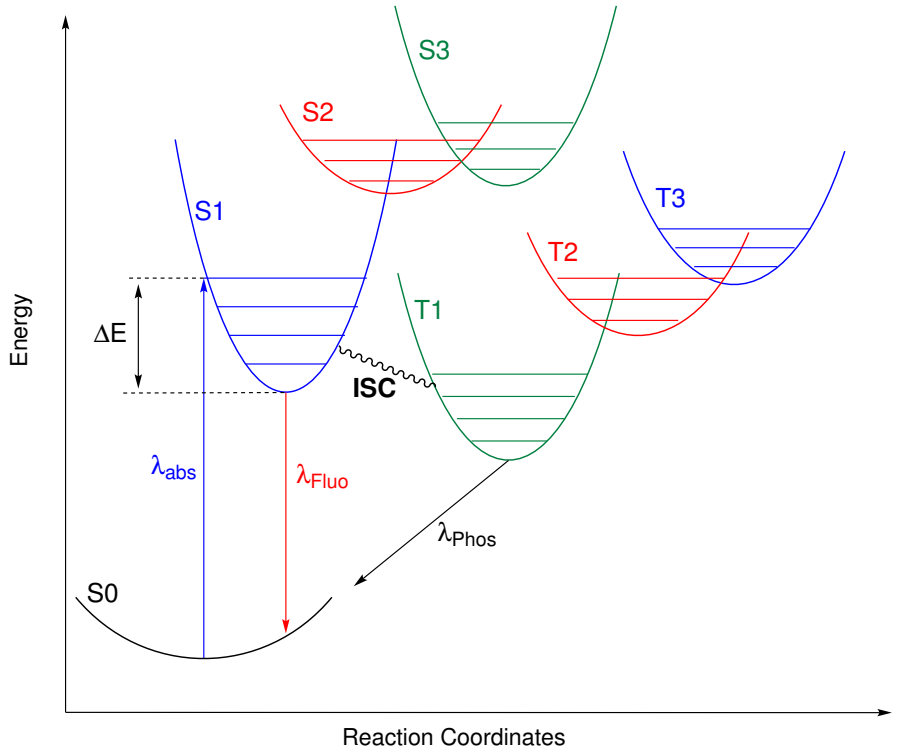

Figure S15 Schematic representation of the Jablonski diagram of **1.** The relative energies of the potential energy surfaces of the different states are based on the TD-DFT optimizations performed at the B3LYP/TZ2P level.

Table S3 Relative diabatic and adiabatic energies ($\Delta E_{vertical}$ and ΔE_{relax} in eV) for the lowest excited states of **1s.** B3LYP/TZ2P results.

	$\Delta E_{vertical}$	ΔE_{relax}
T1	2.758	2.003
T2	2.962	2.560
T3	3.253	2.707
S1	3.291	2.288
S2	3.441	3.089
S3	3.848	3.11

Table S4 Energy (ΔE in eV and nm), oscillator strength (*f*), rotatory strength (R in cgs), electric dipole (D in cgs), absorption dissymmetry factor (g_{abs}), and assignment (in per-cent) of the lowest absorption transitions in **1s** calculated at the PBE0/TZ2P and CASPT2 level.

ΔE	*f*	R(× 10^{-40})	D (× 10^{-40})	g_{abs} (× 10^{3})	Nature[(a)]
			PBE0:		
3.380 (367)	0.404	-22.1	315580	-0.279	HO →LU (84%) HO-1 →LU (14%)
3.540 (350)	0.415	57.6	309706	0.743	HO-1 →LU (84%) HO →LU(14%)
4.014 (309)	0.019	-6.1	13127	-1.865	HO-2 →LU (93%)
4.034 (307)	0.379	-7.2	242234	-0.118	HO-3 →LU (92%)
4.406 (281)	0.527	-67.7	315422	-0.858	HO →LU+1 (93%)
			CASPT2:		
2.884 (430)	0.000	0.0	0	0.000	S0 →T1
2.947 (420)	0.419	-16.3	375399	-0.170	S0 →S1
3.134 (395)	0.128	19.1	108155	0.710	S0 →S2
3.311 (374)	0.000	0.0	0	0.000	S0 →T2
3.692 (336)	0.000	0.0	0	0.000	S0 →T3
3.973 (312)	0.134	7.26	88850	0.330	S0 →S3

(a) Only contributions larger than 5% are given.

Table S5 Energy (ΔE in eV and nm), oscillator strength (*f*), rotatory strength (R in cgs), electric dipole (D in cgs), absorption dissymmetry factor (g_{abs}), and assignment (in per-cent) of the lowest absorption transitions in **1s** calculated at the B3LYP/TZ2P level.

ΔE	*f*	R	D (× 10^{-40})	g_{abs} (× 10^{3})	Nature[(a)]
3.248 (381)	0.308	-21.9	248761	-0.353	HO →LU (95%)
3.425 (362)	0.470	55.7	354011	0.629	HO-1 →LU (95%)
3.817 (325)	0.047	-11.9	32829	-1.448	HO-2 →LU (98%)
3.918 (316)	0.351	0.21	230065	0.003	HO-3 →LU (95%)
4.279 (289)	0.523	-57.0	320478	-0.711	HO →LU+1 (95%)

(a) Only contributions larger than 5% are given.

Table S6 Energy (ΔE in eV and nm), oscillator strength (*f*), rotatory strength (R in cgs), electric dipole (D in cgs), absorption dissymmetry factor (g_{abs}), and assignment (in per-cent) of the lowest absorption transitions in **1S** calculated at the CAMB3LYP/TZ2P level.

ΔE	*f*	R	D (× 10^{-40})	g_{abs} (× 10^{3})	Nature[(a)]
3.671 (337)	0.657	13.6	472054	0.115	HO-1 →LU (71%) HO →LU (24%)
4.037 (307)	0.485	19.6	316714	0.248	HO →LU (65%) HO-1 →LU (23%)
4.348 (285)	0.270	-5.8	163810	-0.142	HO-3 →LU (88%)
4.676 (265)	0.291	-88.2	164217	-2.148	HO →LU+1 (52%) HO-2 →Lu (23%)
4.853 (255)	0.240	20.2	130743	0.671	HO-2 →LU (36%) HO-1 →LU+1 (29%) HO-2 →LU+1 (21%)

(a) Only contributions larger than 5% are given.

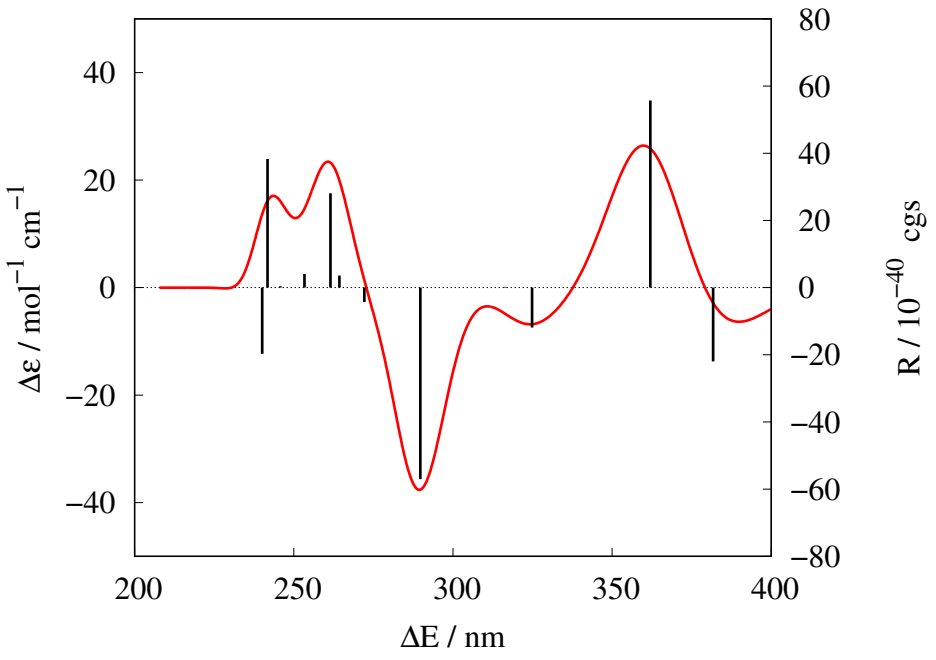

Figure S16 Calculated CD spectra of **1S**, B3LYP/TZ2P results.

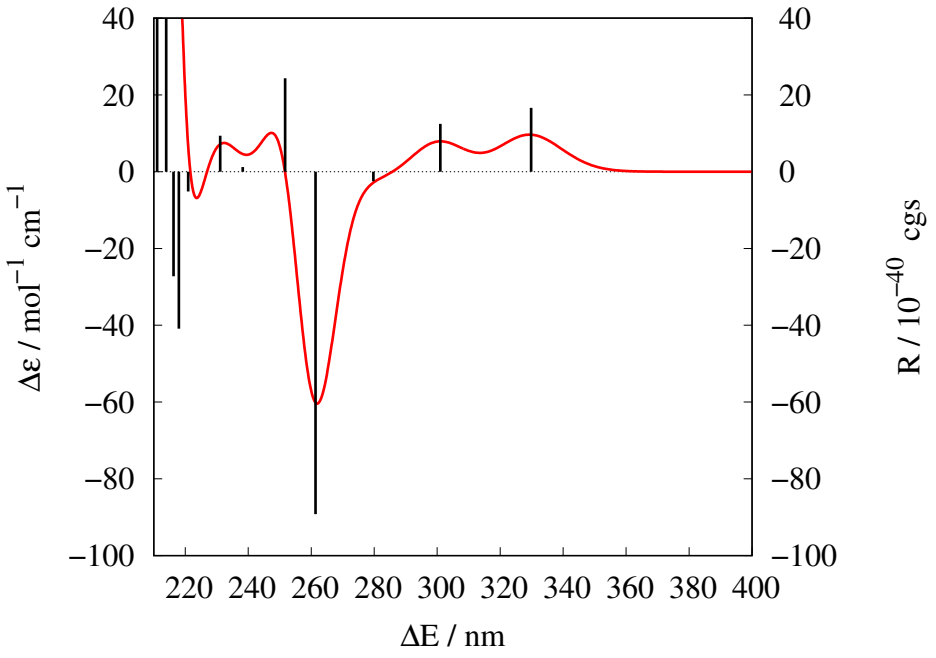

Figure S17 Calculated CD spectra of **1s**, CAM-B3LYP/TZ2P results.

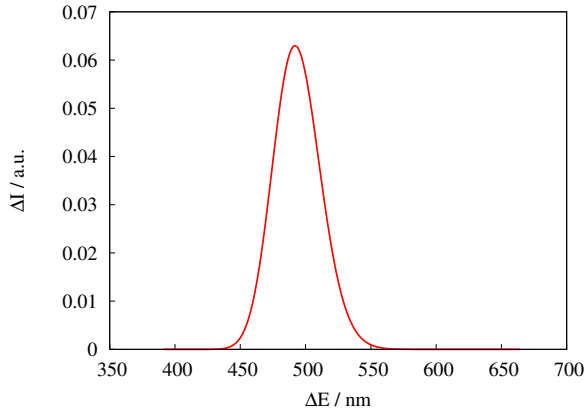

Figure S18 CPL spectrum of **1s** PBE0/TZ2P results. A Gaussian broadening was used with a σ value of 0.13 eV.

NMR Spectra of 6, 1 and 7

2,4-di(2-hydroxyphenyl)benzothiazole (**6**)

^{1}H NMR (400 MHz, $CDCl_3$) spectrum with insert zoom on the aromatic region

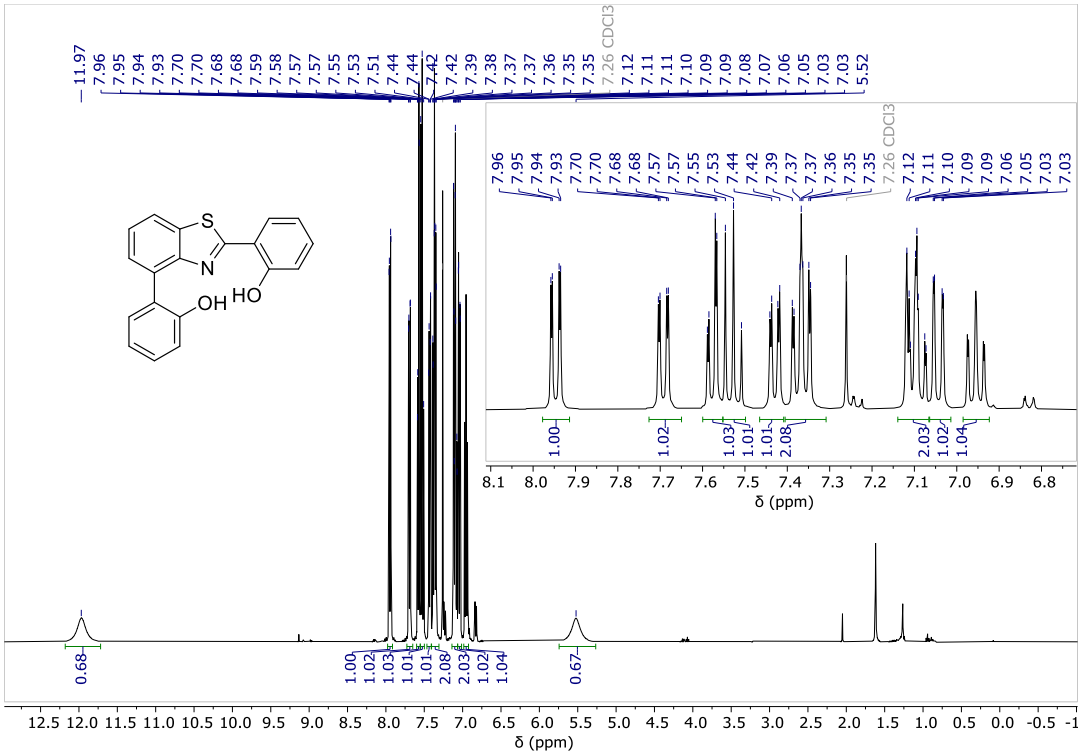

^{13}C{^{1}H} NMR (101 MHz, $CDCl_3$) spectrum

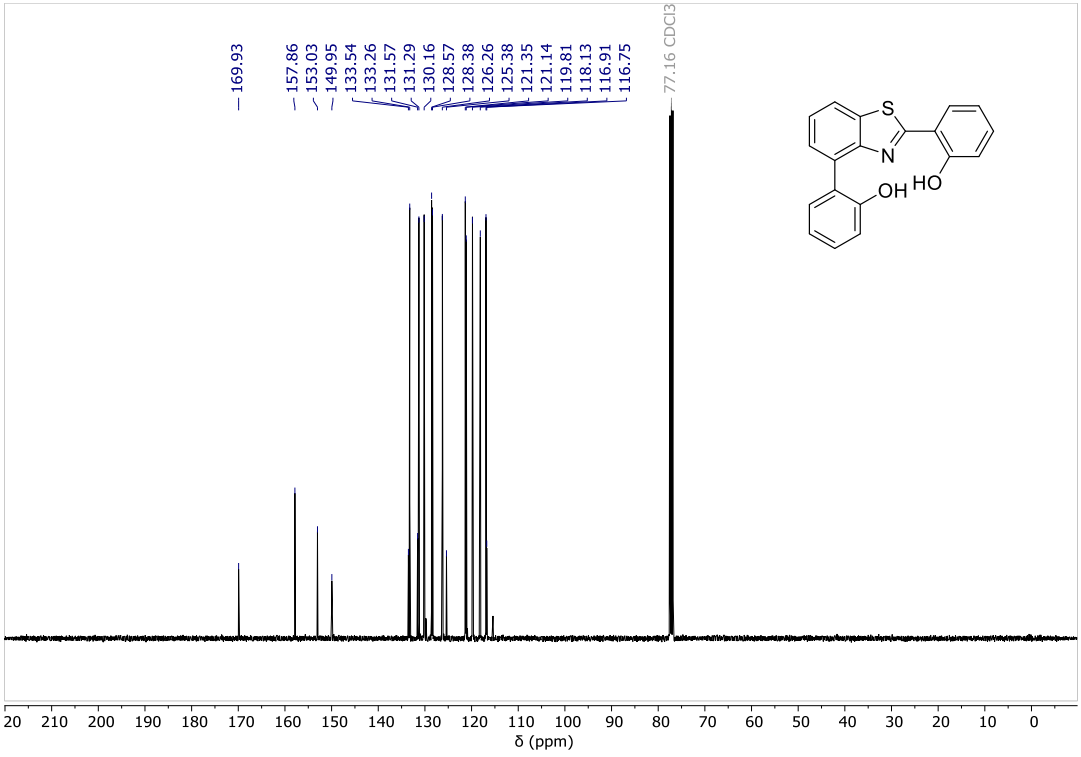

Complex 1

^{1}H NMR (400 MHz, $CDCl_3$) spectrum with inset zoom on the aromatic region

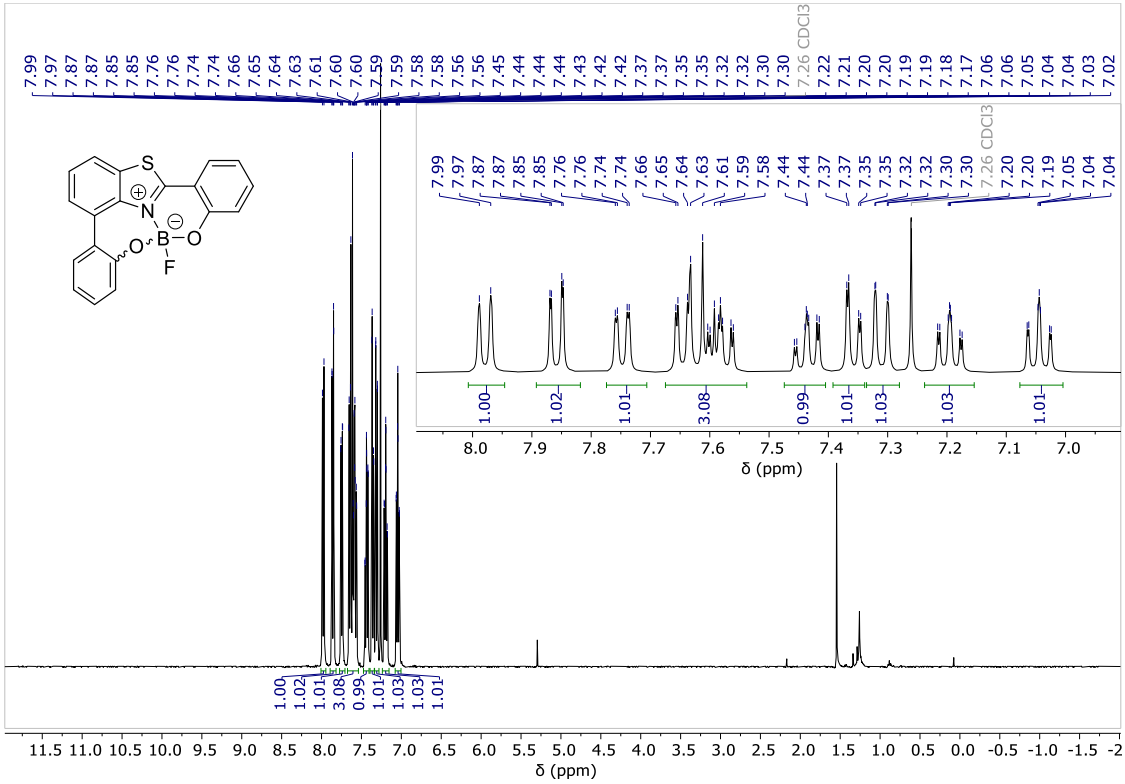

$^{13}C\{^{1}H\}$ NMR (101 MHz, $CDCl_3$) spectrum

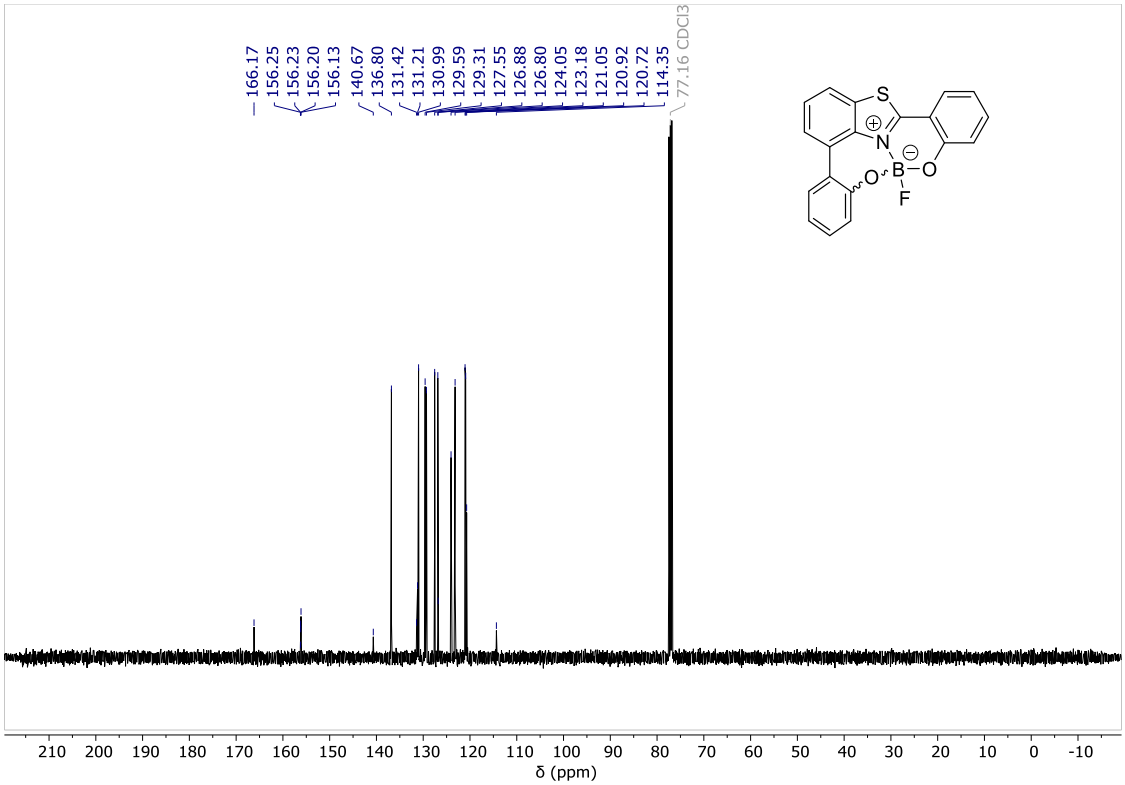

^{19}F NMR (377 MHz, $CDCl_3$) spectrum with inset zoom on peak

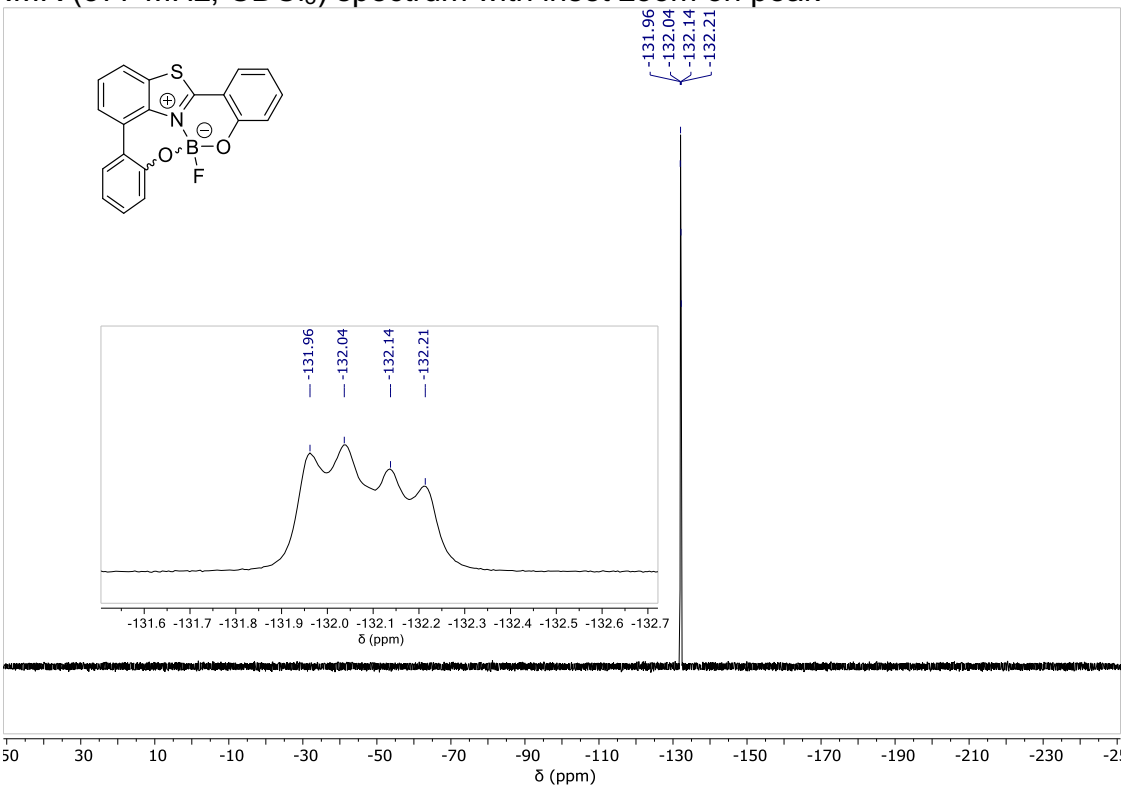

$^{11}B\{^1H\}$ NMR (128 MHz, $CDCl_3$) spectrum with inset zoom on peak

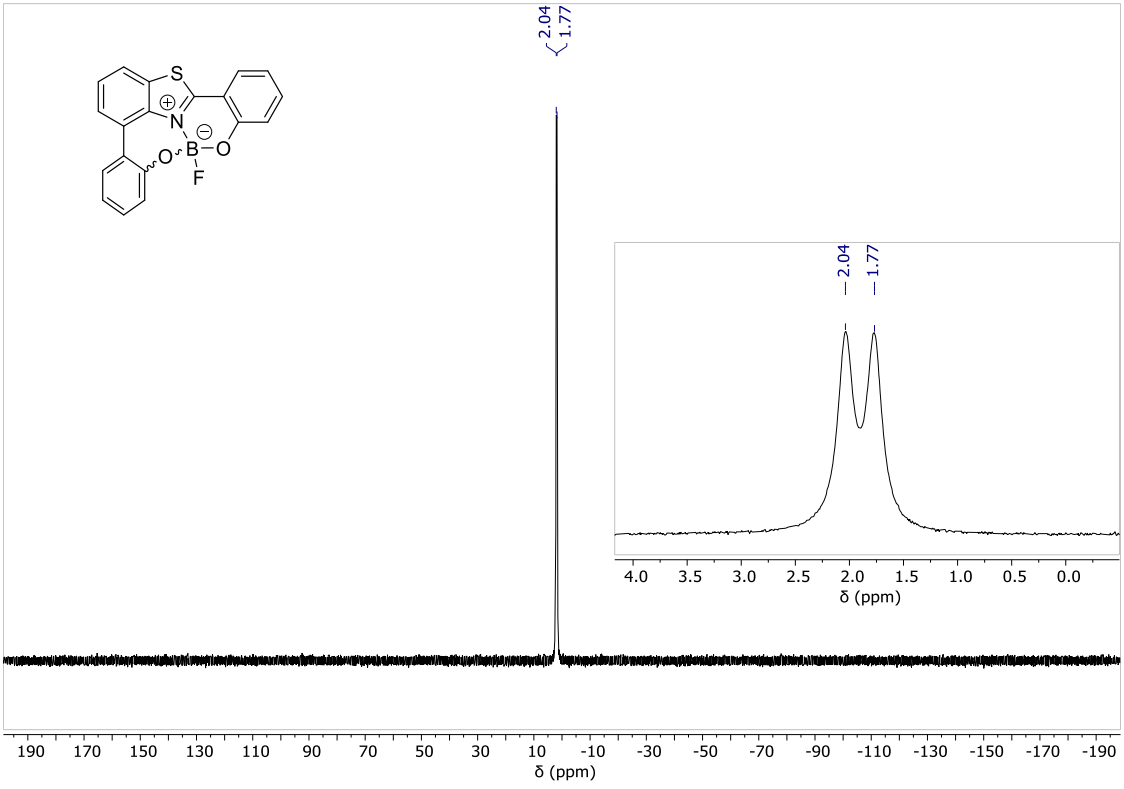

Complex 7

^{1}H NMR (500 MHz, CD_2Cl_2) spectrum with inset zoom on the aromatic region

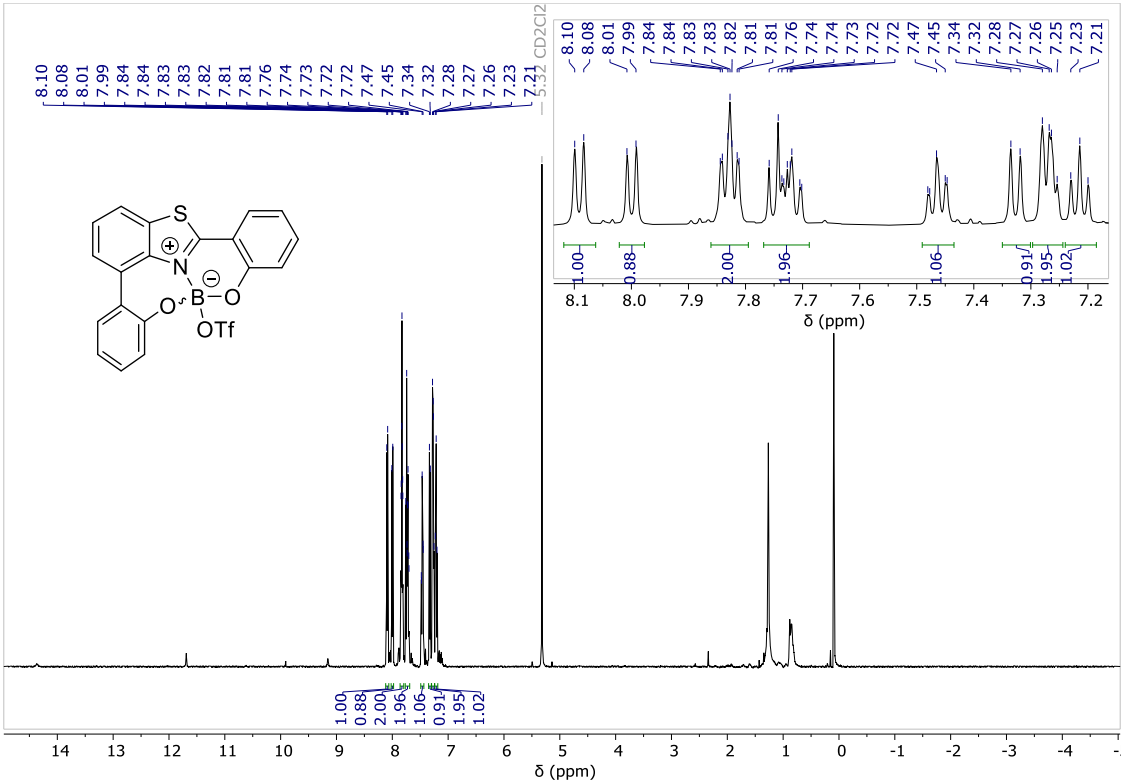

^{13}C{^{1}H} NMR (126 MHz, $CDCl_3$) spectrum with inset zoom on peaks

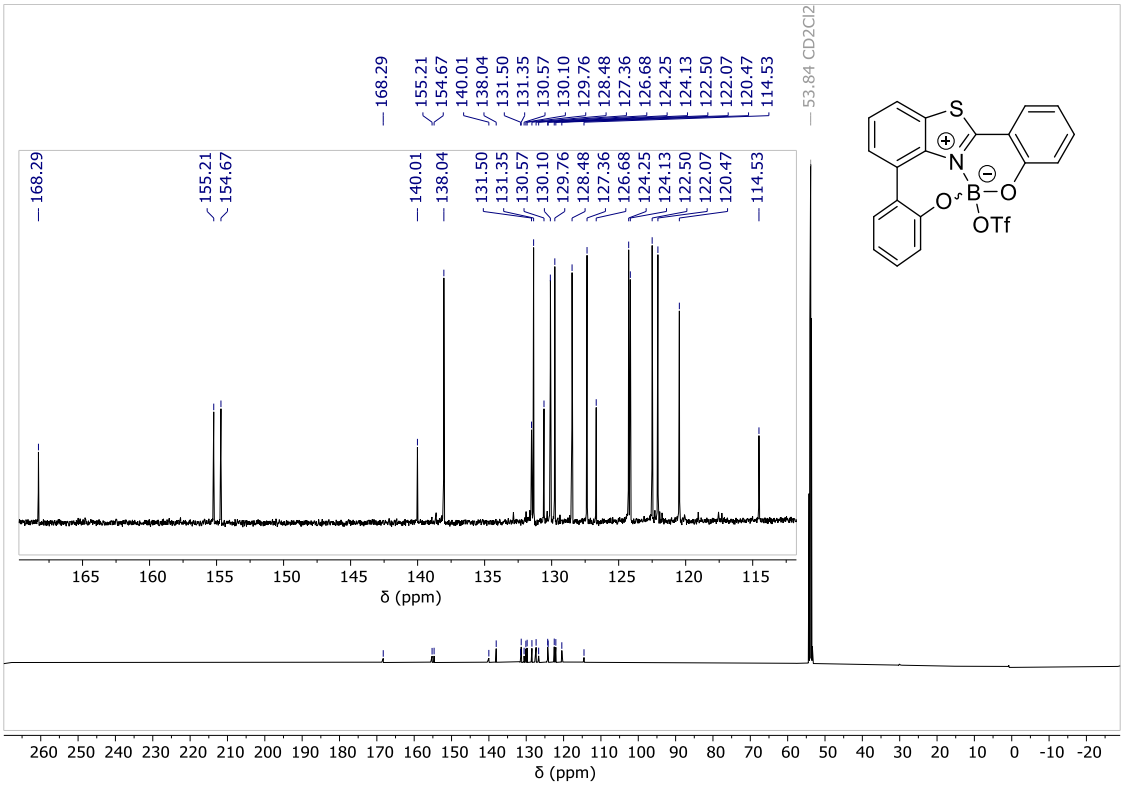

^{19}F NMR (471 MHz, CD_2Cl_2) spectrum with inset zoom on peak

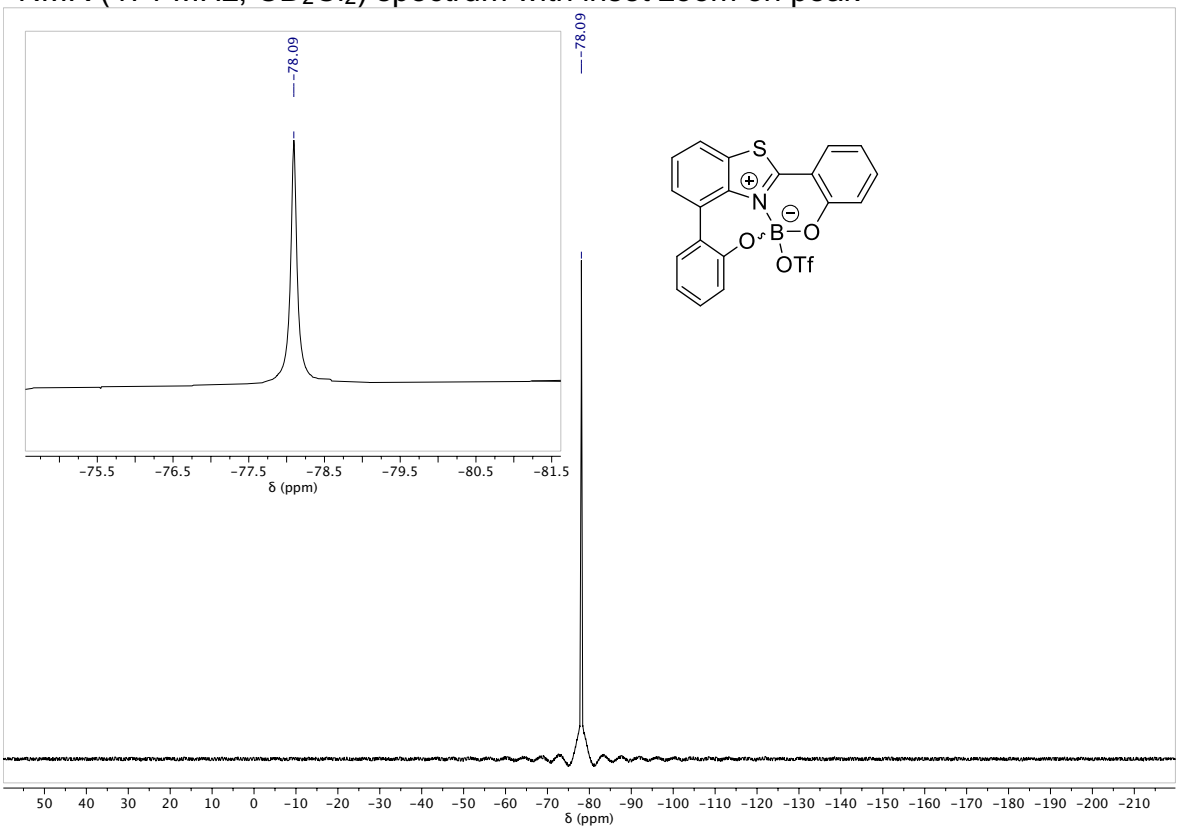

$^{11}B\{^1H\}$ NMR (160 MHz, CD_2Cl_2) spectrum with inset zoom on peak

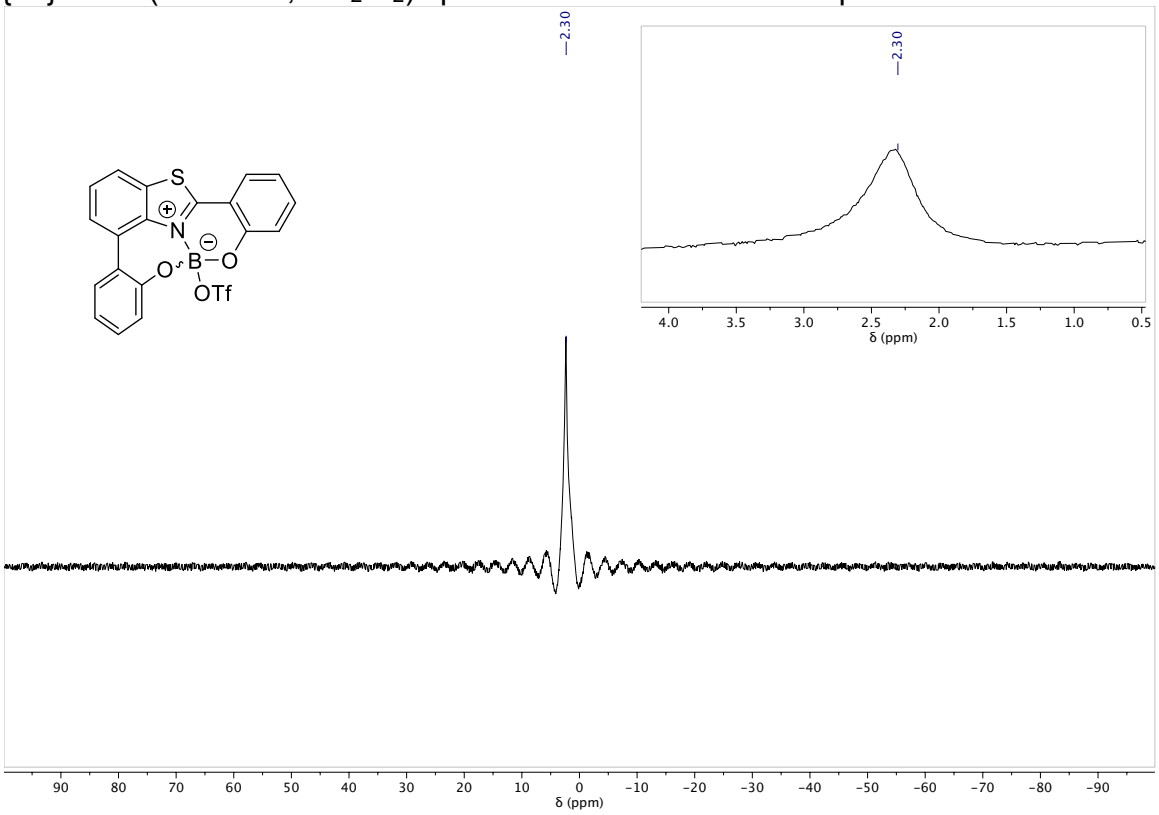

X-ray Data for 2,4-di(2-hydroxyphenyl)benzothiazole (6)

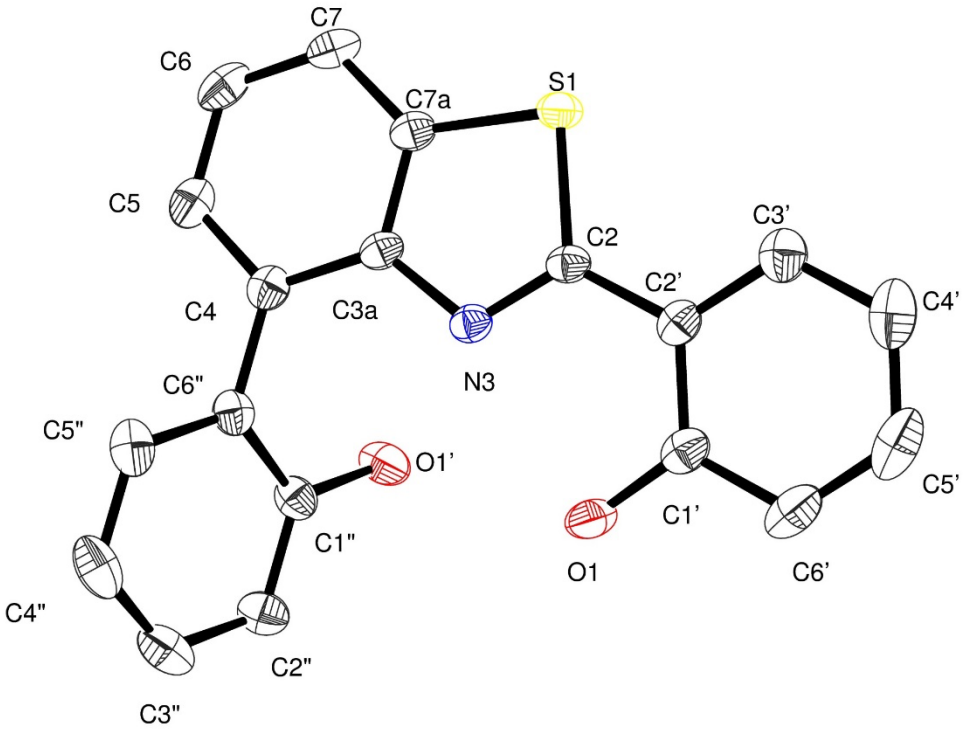

Figure S18

Table S7. Crystal data and structure refinement for OS-1-125-2.

Identification code	OS-1-125-2
Empirical formula	C19 H13 N O2 S
Formula weight	319.36
Temperature	180(2) K
Wavelength	0.71073 A
Crystal system, space group	monoclinic, C 2/c
Unit cell dimensions	a = 10.6417(2) A alpha = 90 deg. b = 13.8292(3) A beta = 93.887(2) deg. c = 20.4893(4) A gamma = 90 deg.
Volume	3008.40(10) A^3
Z, Calculated density	8, 1.410 Mg/m^3
Absorption coefficient	0.224 mm^-1

F(000)	1328
Crystal size	0.38 x 0.24 x 0.2 mm
Theta range for data collection	3.05 to 26.36 deg.
Limiting indices	-13<=h<=13, -17<=k<=17, -25<=l<=25
Reflections collected / unique	29848 / 3072 [R(int) = 0.0298]
Completeness to theta = 26.36	99.8 %
Refinement method	Full-matrix least-squares on F^2
Data / restraints / parameters	3072 / 2 / 216
Goodness-of-fit on F^2	1.057
Final R indices [I>2sigma(I)]	R1 = 0.0312, wR2 = 0.0760
R indices (all data)	R1 = 0.0351, wR2 = 0.0787
Largest diff. peak and hole	0.220 and -0.290 e.A^-3

Table S8. Atomic coordinates (x 10^4) and equivalent isotropic displacement parameters (A^2 x 10^3) for omar2.
U(eq) is defined as one third of the trace of the orthogonalized Uij tensor.

	x	y	z	U(eq)
C(1")	2468(1)	-1016(1)	2319(1)	26(1)
C(2")	2230(2)	-1937(1)	2552(1)	32(1)
C(3")	2916(2)	-2720(1)	2353(1)	36(1)
C(4")	3851(2)	-2588(1)	1926(1)	37(1)
C(5")	4086(1)	-1673(1)	1693(1)	31(1)
C(6")	3396(1)	-871(1)	1875(1)	24(1)
C(4)	3652(1)	99(1)	1604(1)	24(1)
C(5)	4851(1)	502(1)	1646(1)	30(1)
C(6)	5094(1)	1409(1)	1381(1)	33(1)
C(7)	4154(1)	1942(1)	1054(1)	29(1)
C(7A)	2951(1)	1541(1)	993(1)	23(1)
C(3A)	2694(1)	636(1)	1266(1)	21(1)
C(2)	789(1)	952(1)	798(1)	21(1)
C(2')	-532(1)	780(1)	598(1)	23(1)
C(3')	-1200(1)	1369(1)	142(1)	30(1)
C(4')	-2446(2)	1189(1)	-49(1)	38(1)
C(5')	-3048(1)	415(1)	222(1)	42(1)
C(6')	-2420(1)	-177(1)	677(1)	37(1)
C(1')	-1160(1)	-3(1)	869(1)	26(1)
N(3)	1461(1)	331(1)	1148(1)	21(1)
O(1')	1828(1)	-227(1)	2520(1)	35(1)
O(1)	-577(1)	-599(1)	1324(1)	32(1)
S(1)	1591(1)	2002(1)	590(1)	25(1)

Table S9. Bond lengths [A] and angles [deg] for omar2.

C(1")-O(1')	1.3656(16)
C(1")-C(2")	1.3897(19)
C(1")-C(6")	1.4002(19)
C(2")-C(3")	1.383(2)
C(2")-H(2B)	0.9500
C(3")-C(4")	1.381(2)
C(3")-H(3B)	0.9500
C(4")-C(5")	1.382(2)
C(4")-H(4B)	0.9500
C(5")-C(6")	1.3942(19)
C(5")-H(5B)	0.9500
C(6")-C(4)	1.4840(19)
C(4)-C(5)	1.3899(19)
C(4)-C(3A)	1.4055(18)
C(5)-C(6)	1.399(2)
C(5)-H(5)	0.9500
C(6)-C(7)	1.378(2)
C(6)-H(6)	0.9500
C(7)-C(7A)	1.3929(18)
C(7)-H(7)	0.9500
C(7A)-C(3A)	1.4053(18)
C(7A)-S(1)	1.7380(14)
C(3A)-N(3)	1.3834(16)
C(2)-N(3)	1.3005(17)
C(2)-C(2')	1.4572(18)
C(2)-S(1)	1.7514(13)
C(2')-C(3')	1.398(2)
C(2')-C(1')	1.4061(19)
C(3')-C(4')	1.379(2)
C(3')-H(3A)	0.9500
C(4')-C(5')	1.383(2)
C(4')-H(4A)	0.9500
C(5')-C(6')	1.379(2)
C(5')-H(5A)	0.9500
C(6')-C(1')	1.393(2)
C(6')-H(6A)	0.9500
C(1')-O(1)	1.3619(18)
O(1')-H(1A)	0.843(9)
O(1)-H(1)	0.848(9)

O(1')-C(1")-C(2")	121.47(12)
O(1')-C(1")-C(6")	118.01(12)
C(2")-C(1")-C(6")	120.51(12)
C(3")-C(2")-C(1")	120.28(14)
C(3")-C(2")-H(2B)	119.9
C(1")-C(2")-H(2B)	119.9
C(4")-C(3")-C(2")	120.02(14)
C(4")-C(3")-H(3B)	120.0
C(2")-C(3")-H(3B)	120.0
C(3")-C(4")-C(5")	119.67(14)
C(3")-C(4")-H(4B)	120.2
C(5")-C(4")-H(4B)	120.2
C(4")-C(5")-C(6")	121.66(14)
C(4")-C(5")-H(5B)	119.2
C(6")-C(5")-H(5B)	119.2
C(5")-C(6")-C(1")	117.83(13)
C(5")-C(6")-C(4)	120.34(12)
C(1")-C(6")-C(4)	121.82(12)
C(5)-C(4)-C(3A)	116.80(12)
C(5)-C(4)-C(6")	122.01(12)

C(3A)-C(4)-C(6")	121.13(12)
C(4)-C(5)-C(6)	121.91(13)
C(4)-C(5)-H(5)	119.0
C(6)-C(5)-H(5)	119.0
C(7)-C(6)-C(5)	121.43(13)
C(7)-C(6)-H(6)	119.3
C(5)-C(6)-H(6)	119.3
C(6)-C(7)-C(7A)	117.56(13)
C(6)-C(7)-H(7)	121.2
C(7A)-C(7)-H(7)	121.2
C(7)-C(7A)-C(3A)	121.46(12)
C(7)-C(7A)-S(1)	128.86(11)
C(3A)-C(7A)-S(1)	109.68(9)
N(3)-C(3A)-C(7A)	114.19(11)
N(3)-C(3A)-C(4)	124.95(11)
C(7A)-C(3A)-C(4)	120.82(12)
N(3)-C(2)-C(2')	122.11(11)
N(3)-C(2)-S(1)	114.95(10)
C(2')-C(2)-S(1)	122.94(10)
C(3')-C(2')-C(1')	118.67(12)
C(3')-C(2')-C(2)	122.02(12)
C(1')-C(2')-C(2)	119.31(12)
C(4')-C(3')-C(2')	121.30(14)
C(4')-C(3')-H(3A)	119.3
C(2')-C(3')-H(3A)	119.3
C(3')-C(4')-C(5')	119.24(15)
C(3')-C(4')-H(4A)	120.4
C(5')-C(4')-H(4A)	120.4
C(6')-C(5')-C(4')	120.98(14)
C(6')-C(5')-H(5A)	119.5
C(4')-C(5')-H(5A)	119.5
C(5')-C(6')-C(1')	120.09(15)
C(5')-C(6')-H(6A)	120.0
C(1')-C(6')-H(6A)	120.0
O(1)-C(1')-C(6')	118.27(13)
O(1)-C(1')-C(2')	122.01(12)
C(6')-C(1')-C(2')	119.70(14)
C(2)-N(3)-C(3A)	112.03(11)
C(1")-O(1')-H(1A)	110.4(14)
C(1')-O(1)-H(1)	107.5(15)
C(7A)-S(1)-C(2)	89.12(6)

Symmetry transformations used to generate equivalent atoms:

Table S10. Anisotropic displacement parameters (A^2 x 10^3) for omar2. The anisotropic displacement factor exponent takes the form: -2 pi^2 [h^2 a*^2 U11 + ... + 2 h k a* b* U12]

	U11	U22	U33	U23	U13	U12
C(1")	30(1)	24(1)	23(1)	-1(1)	2(1)	3(1)
C(2")	40(1)	28(1)	28(1)	3(1)	4(1)	-2(1)
C(3")	53(1)	23(1)	32(1)	1(1)	-6(1)	2(1)
C(4")	49(1)	32(1)	29(1)	-5(1)	-5(1)	15(1)
C(5")	32(1)	39(1)	23(1)	-2(1)	0(1)	9(1)
C(6")	26(1)	28(1)	19(1)	0(1)	-2(1)	2(1)
C(4)	25(1)	30(1)	18(1)	-2(1)	4(1)	1(1)
C(5)	24(1)	43(1)	23(1)	-2(1)	1(1)	0(1)
C(6)	24(1)	47(1)	27(1)	-6(1)	4(1)	-12(1)
C(7)	31(1)	32(1)	24(1)	-2(1)	7(1)	-11(1)
C(7A)	26(1)	25(1)	20(1)	-2(1)	5(1)	-3(1)
C(3A)	23(1)	24(1)	18(1)	-3(1)	6(1)	-3(1)
C(2)	24(1)	20(1)	20(1)	-1(1)	7(1)	-2(1)
C(2')	22(1)	25(1)	22(1)	-6(1)	5(1)	0(1)
C(3')	29(1)	35(1)	27(1)	-3(1)	3(1)	3(1)
C(4')	31(1)	50(1)	33(1)	-10(1)	-4(1)	10(1)
C(5')	23(1)	55(1)	47(1)	-22(1)	1(1)	-1(1)
C(6')	26(1)	38(1)	48(1)	-13(1)	10(1)	-9(1)
C(1')	25(1)	26(1)	30(1)	-7(1)	8(1)	-2(1)
N(3)	22(1)	21(1)	20(1)	-1(1)	5(1)	-2(1)
O(1')	46(1)	26(1)	35(1)	4(1)	21(1)	7(1)
O(1)	29(1)	29(1)	41(1)	4(1)	10(1)	-7(1)
S(1)	27(1)	22(1)	27(1)	4(1)	4(1)	-3(1)

X-ray Data for Complex 1

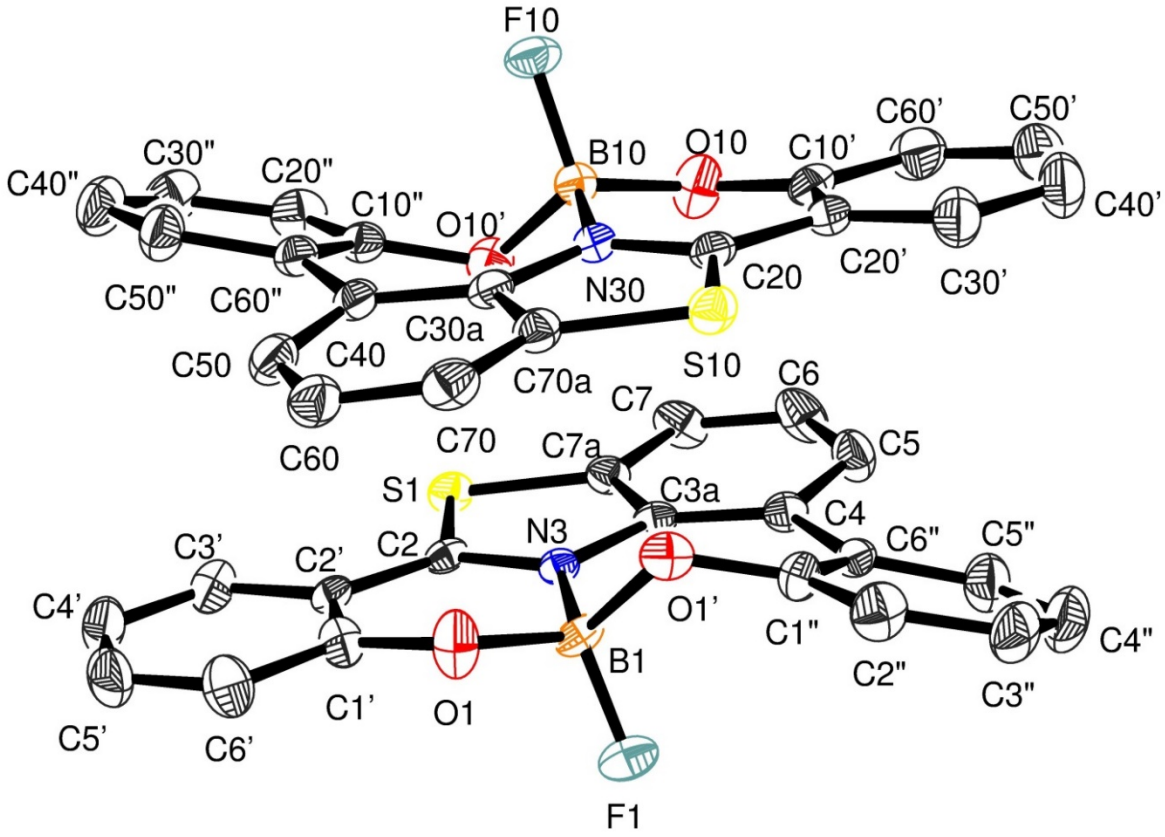

Figure S19a :Asymmetric Unit

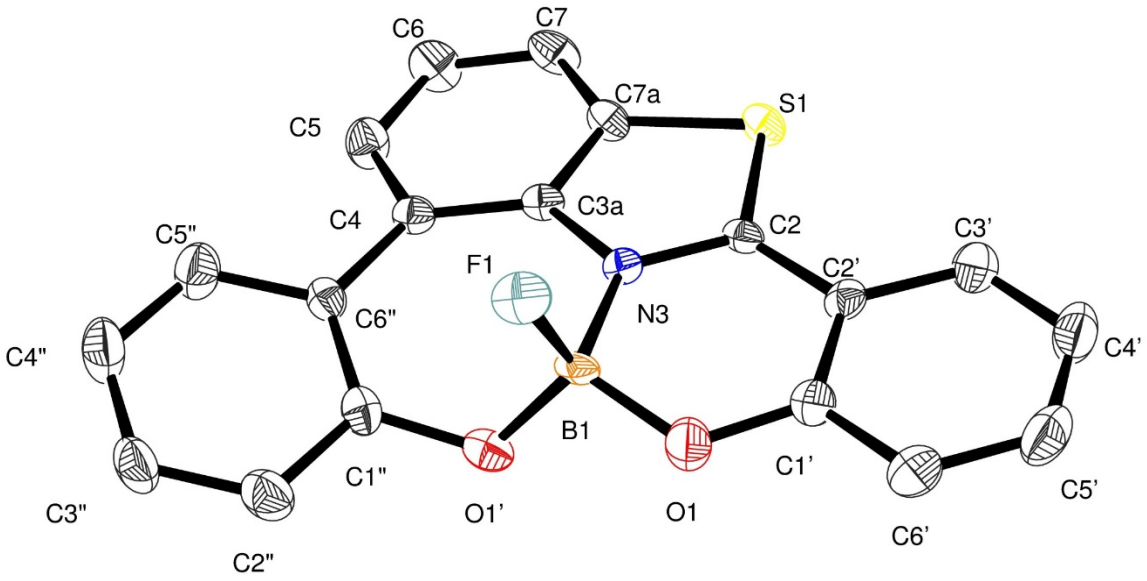

Figure S19b: Single Molecule

Table S11. Crystal data and structure refinement for OS-1-130-3.

Identification code	OS-1-130-3
Empirical formula	C19 H11 B F N O2 S
Formula weight	347.16
Temperature	173(2) K
Wavelength	0.71073 A
Crystal system, space group	monoclinic, P 21/c
Unit cell dimensions	a = 21.6889(15) A alpha = 90 deg. b = 8.3584(6) A beta = 108.741(3) deg. c = 17.3466(12) A gamma = 90 deg.
Volume	2977.9(4) A^3
Z, Calculated density	8, 1.549 Mg/m^3
Absorption coefficient	0.242 mm^-1
F(000)	1424
Crystal size	0.4 x 0.04 x 0.04 mm
Theta range for data collection	5.11 to 26.37 deg.
Limiting indices	-27<=h<=27, -10<=k<=10, -21<=l<=21
Reflections collected / unique	138878 / 6038 [R(int) = 0.0983]

Completeness to theta = 26.37	99.2 %
Refinement method	Full-matrix least-squares on F^2
Data / restraints / parameters	6038 / 0 / 451
Goodness-of-fit on F^2	1.059
Final R indices [I>2sigma(I)]	R1 = 0.0560, wR2 = 0.1321
R indices (all data)	R1 = 0.0896, wR2 = 0.1551
Largest diff. peak and hole	0.887 and -0.341 e.A^-3

Table S12. Atomic coordinates (x 10^4) and equivalent isotropic displacement parameters (A^2 x 10^3) for test2_a.
U(eq) is defined as one third of the trace of the orthogonalized Uij tensor.

	x	y	z	U(eq)
C(2)	2235(1)	9084(3)	2541(2)	17(1)
N(3)	2782(1)	8282(3)	2635(1)	16(1)
S(1)	2108(1)	9527(1)	3440(1)	21(1)
C(4)	3716(2)	7033(4)	3743(2)	20(1)
C(5)	3930(2)	6818(4)	4588(2)	28(1)
C(6)	3618(2)	7446(4)	5103(2)	32(1)
C(7)	3057(2)	8323(4)	4809(2)	28(1)
C(7A)	2818(2)	8534(4)	3974(2)	20(1)
C(3A)	3130(1)	7912(4)	3441(2)	17(1)
C(2')	1799(1)	9491(4)	1745(2)	20(1)
C(1')	1959(2)	8958(4)	1066(2)	25(1)
C(6')	1558(2)	9360(4)	286(2)	33(1)
C(5')	1002(2)	10229(5)	188(2)	37(1)
C(4')	828(2)	10726(5)	854(2)	36(1)
C(3')	1225(2)	10366(4)	1626(2)	30(1)
C(6")	4106(1)	6324(4)	3260(2)	20(1)
C(1")	3862(2)	5935(4)	2430(2)	24(1)
C(2")	4252(2)	5148(4)	2050(2)	32(1)
C(3")	4894(2)	4778(4)	2474(2)	33(1)
C(4")	5150(2)	5221(5)	3275(2)	39(1)
C(5")	4762(2)	5973(5)	3660(2)	33(1)
O(1)	2477(1)	8028(3)	1143(1)	32(1)
O(1')	3224(1)	6229(3)	1956(1)	25(1)
B(1)	3014(2)	7857(4)	1881(2)	19(1)
F(1)	3510(1)	8930(2)	1906(1)	30(1)
S(10)	2871(1)	2528(1)	1578(1)	24(1)
C(20)	2763(1)	2986(4)	2488(2)	21(1)
N(30)	2223(1)	3805(3)	2411(2)	20(1)
C(40)	1293(2)	5113(4)	1325(2)	22(1)
C(50)	1082(2)	5367(4)	487(2)	27(1)
C(60)	1370(2)	4726(4)	-50(2)	31(1)
C(70)	1914(2)	3766(4)	228(2)	28(1)
C(70A)	2165(2)	3561(4)	1067(2)	22(1)
C(30A)	1870(1)	4195(4)	1609(2)	21(1)
C(20')	3209(2)	2568(4)	3277(2)	23(1)
C(10')	3081(2)	3168(4)	3965(2)	27(1)
C(60')	3511(2)	2803(5)	4741(2)	36(1)
C(50')	4046(2)	1848(5)	4806(2)	40(1)
C(40')	4183(2)	1293(5)	4130(2)	41(1)
C(30')	3766(2)	1646(4)	3367(2)	34(1)
C(60")	906(2)	5802(4)	1824(2)	23(1)
C(10")	1148(2)	6153(4)	2649(2)	24(1)
C(20")	762(2)	6927(4)	3040(2)	32(1)
C(30")	126(2)	7349(4)	2621(2)	36(1)
C(40")	-133(2)	6964(5)	1804(2)	35(1)
C(50")	248(2)	6191(4)	1420(2)	30(1)
O(10)	2566(1)	4101(3)	3906(1)	33(1)
O(10')	1780(1)	5847(3)	3108(1)	26(1)
B(10)	2005(2)	4238(4)	3178(2)	22(1)
F(10)	1528(1)	3134(2)	3192(1)	29(1)

Table S13. Bond lengths [A] and angles [deg] for test2_a.

C(2)-N(3)	1.325(4)
C(2)-C(2')	1.441(4)
C(2)-S(1)	1.708(3)
N(3)-C(3A)	1.395(4)
N(3)-B(1)	1.586(4)
S(1)-C(7A)	1.733(3)
C(4)-C(5)	1.401(4)
C(4)-C(3A)	1.414(4)
C(4)-C(6")	1.491(4)
C(5)-C(6)	1.387(5)
C(5)-H(5)	0.9500
C(6)-C(7)	1.369(5)
C(6)-H(6)	0.9500
C(7)-C(7A)	1.385(4)
C(7)-H(7)	0.9500
C(7A)-C(3A)	1.408(4)
C(2')-C(3')	1.401(4)
C(2')-C(1')	1.403(4)
C(1')-O(1)	1.337(4)
C(1')-C(6')	1.395(5)
C(6')-C(5')	1.371(5)
C(6')-H(6')	0.9500
C(5')-C(4')	1.389(5)
C(5')-H(5')	0.9500
C(4')-C(3')	1.373(5)
C(4')-H(4')	0.9500
C(3')-H(3')	0.9500
C(6")-C(5")	1.399(4)
C(6")-C(1")	1.403(4)
C(1")-O(1')	1.386(4)
C(1")-C(2")	1.395(4)
C(2")-C(3")	1.385(5)
C(2")-H(2")	0.9500
C(3")-C(4")	1.371(5)
C(3")-H(3")	0.9500
C(4")-C(5")	1.382(5)
C(4")-H(4")	0.9500
C(5")-H(5")	0.9500
O(1)-B(1)	1.434(4)
O(1')-B(1)	1.427(4)
B(1)-F(1)	1.389(4)
S(10)-C(20)	1.713(3)
S(10)-C(70A)	1.733(3)
C(20)-N(30)	1.326(4)
C(20)-C(20')	1.442(4)
N(30)-C(30A)	1.394(4)
N(30)-B(10)	1.589(4)
C(40)-C(50)	1.392(4)
C(40)-C(30A)	1.414(4)
C(40)-C(60")	1.502(4)
C(50)-C(60)	1.385(5)
C(50)-H(50)	0.9500
C(60)-C(70)	1.379(5)
C(60)-H(60)	0.9500
C(70)-C(70A)	1.390(4)
C(70)-H(70)	0.9500
C(70A)-C(30A)	1.401(4)
C(20')-C(30')	1.400(5)
C(20')-C(10')	1.403(5)
C(10')-O(10)	1.338(4)

C(10')-C(60')	1.403(5)
C(60')-C(50')	1.384(5)
C(60')-H(60')	0.9500
C(50')-C(40')	1.380(6)
C(50')-H(50')	0.9500
C(40')-C(30')	1.374(5)
C(40')-H(40')	0.9500
C(30')-H(30')	0.9500
C(60")-C(10")	1.388(4)
C(60")-C(50")	1.411(4)
C(10")-O(10')	1.371(4)
C(10")-C(20")	1.395(5)
C(20")-C(30")	1.381(5)
C(20")-H(20")	0.9500
C(30")-C(40")	1.384(5)
C(30")-H(30")	0.9500
C(40")-C(50")	1.378(5)
C(40")-H(40")	0.9500
C(50")-H(50")	0.9500
O(10)-B(10)	1.450(4)
O(10')-B(10)	1.423(4)
B(10)-F(10)	1.392(4)

N(3)-C(2)-C(2')	121.5(3)
N(3)-C(2)-S(1)	113.4(2)
C(2')-C(2)-S(1)	125.0(2)
C(2)-N(3)-C(3A)	114.2(2)
C(2)-N(3)-B(1)	121.4(2)
C(3A)-N(3)-B(1)	124.3(2)
C(2)-S(1)-C(7A)	90.45(14)
C(5)-C(4)-C(3A)	114.3(3)
C(5)-C(4)-C(6")	118.6(3)
C(3A)-C(4)-C(6")	127.1(3)
C(6)-C(5)-C(4)	124.0(3)
C(6)-C(5)-H(5)	118.0
C(4)-C(5)-H(5)	118.0
C(7)-C(6)-C(5)	121.5(3)
C(7)-C(6)-H(6)	119.3
C(5)-C(6)-H(6)	119.3
C(6)-C(7)-C(7A)	116.6(3)
C(6)-C(7)-H(7)	121.7
C(7A)-C(7)-H(7)	121.7
C(7)-C(7A)-C(3A)	122.8(3)
C(7)-C(7A)-S(1)	126.2(2)
C(3A)-C(7A)-S(1)	111.0(2)
N(3)-C(3A)-C(7A)	110.8(3)
N(3)-C(3A)-C(4)	128.3(3)
C(7A)-C(3A)-C(4)	120.9(3)
C(3')-C(2')-C(1')	119.3(3)
C(3')-C(2')-C(2)	122.9(3)
C(1')-C(2')-C(2)	117.8(3)
O(1)-C(1')-C(6')	118.6(3)
O(1)-C(1')-C(2')	121.8(3)
C(6')-C(1')-C(2')	119.6(3)
C(5')-C(6')-C(1')	119.8(3)
C(5')-C(6')-H(6')	120.1
C(1')-C(6')-H(6')	120.1
C(6')-C(5')-C(4')	121.3(3)
C(6')-C(5')-H(5')	119.3
C(4')-C(5')-H(5')	119.3
C(3')-C(4')-C(5')	119.5(3)
C(3')-C(4')-H(4')	120.2
C(5')-C(4')-H(4')	120.2

C(4')-C(3')-C(2')	120.5(3)
C(4')-C(3')-H(3')	119.8
C(2')-C(3')-H(3')	119.8
C(5")-C(6")-C(1")	116.7(3)
C(5")-C(6")-C(4)	118.4(3)
C(1")-C(6")-C(4)	124.9(3)
O(1')-C(1")-C(2")	116.4(3)
O(1')-C(1")-C(6")	123.0(3)
C(2")-C(1")-C(6")	120.6(3)
C(3")-C(2")-C(1")	120.9(3)
C(3")-C(2")-H(2")	119.6
C(1")-C(2")-H(2")	119.6
C(4")-C(3")-C(2")	119.2(3)
C(4")-C(3")-H(3")	120.4
C(2")-C(3")-H(3")	120.4
C(3")-C(4")-C(5")	120.1(3)
C(3")-C(4")-H(4")	119.9
C(5")-C(4")-H(4")	119.9
C(4")-C(5")-C(6")	122.4(3)
C(4")-C(5")-H(5")	118.8
C(6")-C(5")-H(5")	118.8
C(1')-O(1)-B(1)	124.3(2)
C(1")-O(1')-B(1)	116.8(2)
F(1)-B(1)-O(1')	113.1(3)
F(1)-B(1)-O(1)	111.3(3)
O(1')-B(1)-O(1)	108.6(3)
F(1)-B(1)-N(3)	106.1(2)
O(1')-B(1)-N(3)	108.3(3)
O(1)-B(1)-N(3)	109.3(2)
C(20)-S(10)-C(70A)	89.98(15)
N(30)-C(20)-C(20')	121.5(3)
N(30)-C(20)-S(10)	113.7(2)
C(20')-C(20)-S(10)	124.8(2)
C(20)-N(30)-C(30A)	113.9(3)
C(20)-N(30)-B(10)	121.6(3)
C(30A)-N(30)-B(10)	124.5(2)
C(50)-C(40)-C(30A)	113.8(3)
C(50)-C(40)-C(60")	119.1(3)
C(30A)-C(40)-C(60")	127.1(3)
C(60)-C(50)-C(40)	125.1(3)
C(60)-C(50)-H(50)	117.5
C(40)-C(50)-H(50)	117.5
C(70)-C(60)-C(50)	120.6(3)
C(70)-C(60)-H(60)	119.7
C(50)-C(60)-H(60)	119.7
C(60)-C(70)-C(70A)	116.2(3)
C(60)-C(70)-H(70)	121.9
C(70A)-C(70)-H(70)	121.9
C(70)-C(70A)-C(30A)	123.1(3)
C(70)-C(70A)-S(10)	125.5(2)
C(30A)-C(70A)-S(10)	111.4(2)
N(30)-C(30A)-C(70A)	111.0(3)
N(30)-C(30A)-C(40)	128.0(3)
C(70A)-C(30A)-C(40)	121.0(3)
C(30')-C(20')-C(10')	120.1(3)
C(30')-C(20')-C(20)	122.1(3)
C(10')-C(20')-C(20)	117.7(3)
O(10)-C(10')-C(60')	118.8(3)
O(10)-C(10')-C(20')	122.1(3)
C(60')-C(10')-C(20')	119.1(3)
C(50')-C(60')-C(10')	119.1(4)
C(50')-C(60')-H(60')	120.5
C(10')-C(60')-H(60')	120.5

C(40')-C(50')-C(60')	122.0(3)
C(40')-C(50')-H(50')	119.0
C(60')-C(50')-H(50')	119.0
C(30')-C(40')-C(50')	119.5(4)
C(30')-C(40')-H(40')	120.3
C(50')-C(40')-H(40')	120.3
C(40')-C(30')-C(20')	120.2(4)
C(40')-C(30')-H(30')	119.9
C(20')-C(30')-H(30')	119.9
C(10")-C(60")-C(50")	116.8(3)
C(10")-C(60")-C(40)	125.4(3)
C(50")-C(60")-C(40)	117.8(3)
O(10')-C(10")-C(60")	122.4(3)
O(10')-C(10")-C(20")	116.7(3)
C(60")-C(10")-C(20")	120.8(3)
C(30")-C(20")-C(10")	121.1(3)
C(30")-C(20")-H(20")	119.4
C(10")-C(20")-H(20")	119.4
C(20")-C(30")-C(40")	119.2(3)
C(20")-C(30")-H(30")	120.4
C(40")-C(30")-H(30")	120.4
C(50")-C(40")-C(30")	119.6(3)
C(50")-C(40")-H(40")	120.2
C(30")-C(40")-H(40")	120.2
C(40")-C(50")-C(60")	122.4(3)
C(40")-C(50")-H(50")	118.8
C(60")-C(50")-H(50")	118.8
C(10')-O(10)-B(10)	123.9(3)
C(10")-O(10')-B(10)	118.5(2)
F(10)-B(10)-O(10')	113.0(3)
F(10)-B(10)-O(10)	110.7(3)
O(10')-B(10)-O(10)	108.5(3)
F(10)-B(10)-N(30)	106.6(3)
O(10')-B(10)-N(30)	109.3(3)
O(10)-B(10)-N(30)	108.7(3)

Symmetry transformations used to generate equivalent atoms:

Table S14. Anisotropic displacement parameters (A^2 x 10^3) for test2_a.
The anisotropic displacement factor exponent takes the form:
-2 pi^2 [h^2 a*^2 U11 + ... + 2 h k a* b* U12]

	U11	U22	U33	U23	U13	U12
C(2)	17(1)	16(2)	21(2)	-4(1)	11(1)	-3(1)
N(3)	17(1)	18(1)	15(1)	-1(1)	7(1)	-2(1)
S(1)	23(1)	23(1)	23(1)	-1(1)	14(1)	1(1)
C(4)	22(2)	20(2)	20(2)	-1(1)	9(1)	-2(1)
C(5)	29(2)	34(2)	22(2)	6(1)	8(1)	7(2)
C(6)	45(2)	37(2)	17(2)	7(1)	12(2)	9(2)
C(7)	42(2)	27(2)	21(2)	0(1)	19(2)	5(2)
C(7A)	24(2)	20(2)	22(2)	1(1)	13(1)	1(1)
C(3A)	21(2)	19(2)	15(1)	-1(1)	10(1)	-3(1)
C(2')	15(1)	19(2)	23(2)	-1(1)	5(1)	-5(1)
C(1')	25(2)	24(2)	23(2)	0(1)	5(1)	3(1)
C(6')	35(2)	38(2)	22(2)	-1(2)	4(2)	3(2)
C(5')	31(2)	38(2)	30(2)	7(2)	-5(2)	-1(2)
C(4')	22(2)	37(2)	42(2)	4(2)	1(2)	2(2)
C(3')	21(2)	33(2)	33(2)	-3(2)	7(1)	0(1)

C(6")	19(2)	18(2)	26(2)	1(1)	10(1)	-1(1)
C(1")	20(2)	26(2)	29(2)	1(1)	10(1)	3(1)
C(2")	34(2)	35(2)	31(2)	-4(2)	16(2)	3(2)
C(3")	27(2)	39(2)	38(2)	-2(2)	18(2)	8(2)
C(4")	24(2)	51(2)	45(2)	4(2)	13(2)	10(2)
C(5")	26(2)	43(2)	28(2)	4(2)	7(1)	6(2)
O(1)	29(1)	48(2)	20(1)	-3(1)	7(1)	12(1)
O(1')	31(1)	23(1)	26(1)	-4(1)	14(1)	-1(1)
B(1)	18(2)	22(2)	20(2)	-9(1)	13(1)	-4(1)
F(1)	30(1)	34(1)	31(1)	-3(1)	18(1)	-9(1)
S(10)	23(1)	25(1)	28(1)	-1(1)	12(1)	1(1)
C(20)	20(2)	19(2)	26(2)	1(1)	10(1)	-4(1)
N(30)	17(1)	19(1)	22(1)	1(1)	6(1)	-2(1)
C(40)	18(2)	20(2)	29(2)	0(1)	8(1)	-3(1)
C(50)	20(2)	34(2)	29(2)	1(2)	9(1)	-2(1)
C(60)	26(2)	41(2)	27(2)	6(2)	10(1)	-2(2)
C(70)	29(2)	35(2)	23(2)	-2(1)	14(1)	-4(2)
C(70A)	22(2)	20(2)	25(2)	-1(1)	8(1)	-3(1)
C(30A)	19(2)	23(2)	20(2)	0(1)	7(1)	-6(1)
C(20')	19(2)	19(2)	28(2)	1(1)	5(1)	-4(1)
C(10')	20(2)	29(2)	30(2)	3(1)	6(1)	-7(1)
C(60')	33(2)	44(2)	29(2)	4(2)	6(2)	-8(2)
C(50')	33(2)	43(2)	35(2)	11(2)	0(2)	-1(2)
C(40')	28(2)	38(2)	48(2)	5(2)	1(2)	7(2)
C(30')	28(2)	31(2)	37(2)	-1(2)	4(2)	3(2)
C(60")	20(2)	19(2)	30(2)	1(1)	10(1)	-1(1)
C(10")	22(2)	18(2)	31(2)	0(1)	7(1)	-3(1)
C(20")	36(2)	31(2)	33(2)	-4(2)	16(2)	-1(2)
C(30")	30(2)	36(2)	50(2)	-9(2)	23(2)	2(2)
C(40")	23(2)	42(2)	43(2)	0(2)	13(2)	5(2)
C(50")	21(2)	38(2)	30(2)	2(2)	9(1)	4(2)
O(10)	27(1)	49(2)	22(1)	-5(1)	7(1)	4(1)
O(10')	25(1)	24(1)	30(1)	-4(1)	7(1)	-1(1)
B(10)	21(2)	23(2)	22(2)	2(1)	7(1)	-1(1)
F(10)	28(1)	27(1)	40(1)	1(1)	20(1)	-5(1)

X-ray Data for Complex 7

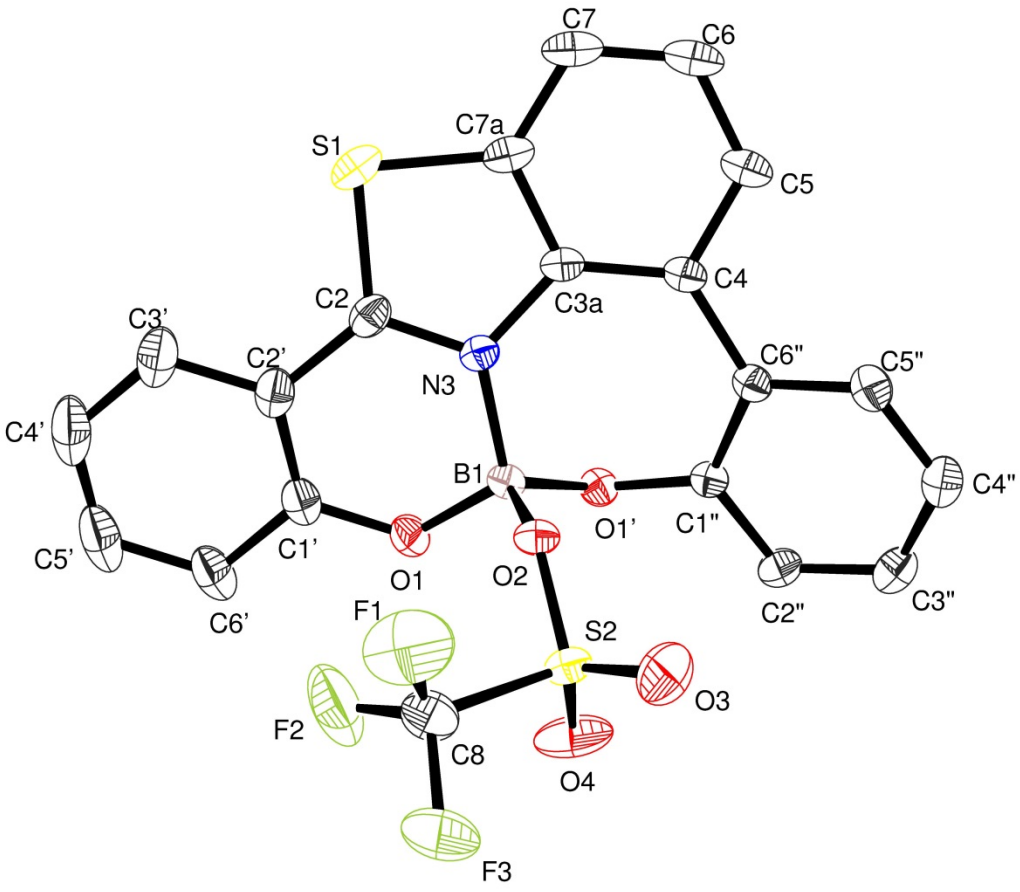

Figure S20: Asymmetric Unit

Table S15. Crystal data and structure refinement for borenium-O.

Identification code	borenium-O
Empirical formula	C20 H11 B F3 N O5 S2
Formula weight	477.23
Temperature	193(2) K
Wavelength	0.71073 A
Crystal system, space group	Triclinic, P -1
Unit cell dimensions	a = 9.7669(8) A alpha = 78.238(4) deg. b = 9.7700(9) A beta = 71.095(3) deg. c = 10.9230(10) A gamma = 83.741(3) deg.

Volume	964.33(15) A^3
Z, Calculated density	2, 1.644 Mg/m^3
Absorption coefficient	0.341 mm^-1
F(000)	484
Crystal size	0.400 x 0.280 x 0.080 mm
Theta range for data collection	3.177 to 37.840 deg.
Limiting indices	-16<=h<=16, -16<=k<=16, -18<=l<=18
Reflections collected / unique	88021 / 10264 [R(int) = 0.0466]
Completeness to theta = 25.242	98.9 %
Refinement method	Full-matrix least-squares on F^2
Data / restraints / parameters	10264 / 0 / 289
Goodness-of-fit on F^2	1.048
Final R indices [I>2sigma(I)]	R1 = 0.0461, wR2 = 0.1286
R indices (all data)	R1 = 0.0565, wR2 = 0.1361
Largest diff. peak and hole	0.569 and -0.484 e.A^-3

Table S16. Atomic coordinates (x 10^4) and equivalent isotropic displacement parameters (A^2 x 10^3) for borenium-O.
U(eq) is defined as one third of the trace of the orthogonalized Uij tensor.

	x	y	z	U(eq)
C(1")	8625(1)	7761(1)	4352(1)	19(1)
C(1')	9040(1)	4134(1)	7907(1)	26(1)
C(2')	8207(1)	3137(1)	7752(1)	27(1)
C(2")	9111(1)	9105(1)	4103(1)	25(1)
C(2)	7642(1)	3467(1)	6659(1)	24(1)
C(3')	8056(2)	1822(1)	8585(1)	38(1)
C(3")	8504(1)	10211(1)	3401(1)	30(1)
C(3A)	7218(1)	4843(1)	4851(1)	20(1)
C(4")	7382(1)	9968(1)	2965(1)	30(1)
C(4')	8711(2)	1519(2)	9558(1)	48(1)
C(4)	7153(1)	6033(1)	3892(1)	21(1)
C(5")	6931(1)	8618(1)	3177(1)	27(1)
C(5)	6649(1)	5802(1)	2890(1)	29(1)
C(5')	9527(2)	2521(2)	9714(1)	47(1)
C(6')	9705(1)	3819(2)	8896(1)	36(1)
C(6)	6167(1)	4519(1)	2859(1)	34(1)
C(6")	7565(1)	7466(1)	3839(1)	21(1)
C(7)	6177(1)	3375(1)	3830(1)	33(1)
C(7A)	6738(1)	3554(1)	4807(1)	26(1)
C(8)	6241(2)	7253(2)	9331(1)	42(1)
B(1)	8428(1)	5925(1)	6242(1)	20(1)
F(1)	4988(2)	6685(2)	9585(1)	76(1)
F(2)	7162(2)	6284(2)	9678(1)	79(1)
F(3)	6015(2)	8233(1)	10062(1)	67(1)
N(3)	7709(1)	4740(1)	5936(1)	20(1)
O(1)	9271(1)	5381(1)	7091(1)	26(1)
O(1')	9275(1)	6746(1)	5078(1)	20(1)
O(2)	7046(1)	6771(1)	6974(1)	21(1)
O(3)	5812(1)	8983(1)	7350(1)	48(1)
O(4)	8300(1)	8550(1)	7429(1)	49(1)
S(1)	6943(1)	2277(1)	6100(1)	30(1)
S(2)	6941(1)	8036(1)	7596(1)	24(1)

Table S17. Bond lengths [A] and angles [deg] for borenium-O.

C(1")-O(1')	1.3730(11)
C(1")-C(2")	1.3885(13)
C(1")-C(6")	1.4056(12)
C(1')-O(1)	1.3472(13)
C(1')-C(6')	1.3995(15)
C(1')-C(2')	1.4026(16)
C(2')-C(3')	1.4067(15)
C(2')-C(2)	1.4373(15)
C(2")-C(3")	1.3871(15)
C(2")-H(2")	0.9500
C(2)-N(3)	1.3264(12)
C(2)-S(1)	1.7098(10)
C(3')-C(4')	1.377(2)
C(3')-H(3')	0.9500
C(3")-C(4")	1.3877(17)
C(3")-H(3")	0.9500
C(3A)-N(3)	1.3978(12)
C(3A)-C(7A)	1.4056(13)
C(3A)-C(4)	1.4094(13)
C(4")-C(5")	1.3868(16)
C(4")-H(4")	0.9500
C(4')-C(5')	1.396(3)
C(4')-H(4')	0.9500
C(4)-C(5)	1.4017(13)
C(4)-C(6")	1.4829(13)
C(5")-C(6")	1.4070(13)
C(5")-H(5")	0.9500
C(5)-C(6)	1.3962(16)
C(5)-H(5)	0.9500
C(5')-C(6')	1.387(2)
C(5')-H(5')	0.9500
C(6')-H(6')	0.9500
C(6)-C(7)	1.377(2)
C(6)-H(6)	0.9500
C(7)-C(7A)	1.3948(15)
C(7)-H(7)	0.9500
C(7A)-S(1)	1.7324(12)
C(8)-F(2)	1.3182(19)
C(8)-F(1)	1.322(2)
C(8)-F(3)	1.3244(15)
C(8)-S(2)	1.8242(13)
B(1)-O(1')	1.4105(12)
B(1)-O(1)	1.4215(12)
B(1)-N(3)	1.5589(12)
B(1)-O(2)	1.5719(12)
O(2)-S(2)	1.5059(7)
O(3)-S(2)	1.4184(10)
O(4)-S(2)	1.4140(10)
O(1')-C(1")-C(2")	116.30(8)
O(1')-C(1")-C(6")	122.51(8)

C(2")-C(1")-C(6")	121.14(8)
O(1)-C(1')-C(6')	118.40(11)
O(1)-C(1')-C(2')	121.75(9)
C(6')-C(1')-C(2')	119.80(10)
C(1')-C(2')-C(3')	119.77(11)
C(1')-C(2')-C(2)	117.71(9)
C(3')-C(2')-C(2)	122.29(11)
C(3")-C(2")-C(1")	120.83(9)
C(3")-C(2")-H(2")	119.6
C(1")-C(2")-H(2")	119.6
N(3)-C(2)-C(2')	121.49(9)
N(3)-C(2)-S(1)	113.84(8)
C(2')-C(2)-S(1)	124.54(7)
C(4')-C(3')-C(2')	120.13(14)
C(4')-C(3')-H(3')	119.9
C(2')-C(3')-H(3')	119.9
C(2")-C(3")-C(4")	119.20(10)
C(2")-C(3")-H(3")	120.4
C(4")-C(3")-H(3")	120.4
N(3)-C(3A)-C(7A)	111.09(8)
N(3)-C(3A)-C(4)	128.01(8)
C(7A)-C(3A)-C(4)	120.90(8)
C(5")-C(4")-C(3")	119.84(10)
C(5")-C(4")-H(4")	120.1
C(3")-C(4")-H(4")	120.1
C(3')-C(4')-C(5')	119.81(12)
C(3')-C(4')-H(4')	120.1
C(5')-C(4')-H(4')	120.1
C(5)-C(4)-C(3A)	114.95(9)
C(5)-C(4)-C(6")	118.15(9)
C(3A)-C(4)-C(6")	126.90(8)
C(4")-C(5")-C(6")	122.22(9)
C(4")-C(5")-H(5")	118.9
C(6")-C(5")-H(5")	118.9
C(6)-C(5)-C(4)	123.63(11)
C(6)-C(5)-H(5)	118.2
C(4)-C(5)-H(5)	118.2
C(6')-C(5')-C(4')	121.11(13)
C(6')-C(5')-H(5')	119.4
C(4')-C(5')-H(5')	119.4
C(5')-C(6')-C(1')	119.38(14)
C(5')-C(6')-H(6')	120.3
C(1')-C(6')-H(6')	120.3
C(7)-C(6)-C(5)	121.04(10)
C(7)-C(6)-H(6)	119.5
C(5)-C(6)-H(6)	119.5
C(1")-C(6")-C(5")	116.50(8)
C(1")-C(6")-C(4)	124.17(8)
C(5")-C(6")-C(4)	119.24(8)
C(6)-C(7)-C(7A)	116.67(10)
C(6)-C(7)-H(7)	121.7
C(7A)-C(7)-H(7)	121.7
C(7)-C(7A)-C(3A)	122.68(10)
C(7)-C(7A)-S(1)	126.17(8)

C(3A)-C(7A)-S(1)	111.15(8)
F(2)-C(8)-F(1)	108.91(15)
F(2)-C(8)-F(3)	108.71(13)
F(1)-C(8)-F(3)	107.49(13)
F(2)-C(8)-S(2)	111.13(10)
F(1)-C(8)-S(2)	110.88(11)
F(3)-C(8)-S(2)	109.63(11)
O(1')-B(1)-O(1)	110.46(8)
O(1')-B(1)-N(3)	111.51(7)
O(1)-B(1)-N(3)	111.67(8)
O(1')-B(1)-O(2)	111.92(7)
O(1)-B(1)-O(2)	110.37(7)
N(3)-B(1)-O(2)	100.58(7)
C(2)-N(3)-C(3A)	113.70(8)
C(2)-N(3)-B(1)	120.58(8)
C(3A)-N(3)-B(1)	125.42(7)
C(1')-O(1)-B(1)	122.71(8)
C(1")-O(1')-B(1)	120.23(7)
S(2)-O(2)-B(1)	129.49(6)
C(2)-S(1)-C(7A)	90.22(5)
O(4)-S(2)-O(3)	119.52(8)
O(4)-S(2)-O(2)	113.69(5)
O(3)-S(2)-O(2)	110.36(6)
O(4)-S(2)-C(8)	105.89(8)
O(3)-S(2)-C(8)	104.75(7)
O(2)-S(2)-C(8)	100.20(5)

Symmetry transformations used to generate equivalent atoms:

Table S18. Anisotropic displacement parameters (A^2 x 10^3) for borenium-O.

The anisotropic displacement factor exponent takes the form:

-2 pi^2 [h^2 a*^2 U11 + ... + 2 h k a* b* U12]

	U11	U22	U33	U23	U13	U12
C(1")	18(1)	21(1)	19(1)	-4(1)	-5(1)	-2(1)
C(1')	26(1)	29(1)	21(1)	-4(1)	-6(1)	6(1)
C(2')	29(1)	24(1)	23(1)	-2(1)	-2(1)	4(1)
C(2")	25(1)	22(1)	29(1)	-5(1)	-7(1)	-5(1)
C(2)	23(1)	19(1)	25(1)	-4(1)	-2(1)	-1(1)
C(3')	46(1)	28(1)	30(1)	3(1)	-3(1)	4(1)
C(3")	32(1)	22(1)	33(1)	-3(1)	-7(1)	-3(1)
C(3A)	19(1)	22(1)	23(1)	-9(1)	-5(1)	-2(1)
C(4")	32(1)	26(1)	29(1)	0(1)	-9(1)	2(1)
C(4')	60(1)	39(1)	31(1)	7(1)	-9(1)	12(1)
C(4)	20(1)	26(1)	20(1)	-7(1)	-6(1)	-3(1)
C(5")	25(1)	30(1)	26(1)	-3(1)	-10(1)	0(1)
C(5)	29(1)	38(1)	26(1)	-12(1)	-12(1)	-5(1)
C(5')	53(1)	53(1)	27(1)	2(1)	-14(1)	17(1)
C(6')	37(1)	45(1)	25(1)	-6(1)	-13(1)	11(1)
C(6)	33(1)	45(1)	35(1)	-19(1)	-13(1)	-7(1)
C(6")	20(1)	24(1)	19(1)	-4(1)	-6(1)	-3(1)
C(7)	29(1)	35(1)	42(1)	-21(1)	-11(1)	-5(1)
C(7A)	23(1)	24(1)	33(1)	-12(1)	-6(1)	-4(1)
C(8)	57(1)	42(1)	24(1)	-14(1)	-5(1)	1(1)
B(1)	19(1)	21(1)	19(1)	-5(1)	-7(1)	-1(1)
F(1)	75(1)	83(1)	50(1)	-19(1)	24(1)	-39(1)
F(2)	122(1)	77(1)	32(1)	-11(1)	-30(1)	41(1)
F(3)	98(1)	68(1)	39(1)	-36(1)	-14(1)	8(1)
N(3)	20(1)	18(1)	21(1)	-5(1)	-5(1)	-2(1)
O(1)	26(1)	28(1)	25(1)	-3(1)	-13(1)	-1(1)
O(1')	18(1)	23(1)	21(1)	-3(1)	-6(1)	-3(1)
O(2)	20(1)	23(1)	22(1)	-9(1)	-5(1)	-1(1)
O(3)	55(1)	33(1)	57(1)	-13(1)	-22(1)	19(1)
O(4)	36(1)	51(1)	64(1)	-31(1)	-4(1)	-19(1)
S(1)	30(1)	19(1)	41(1)	-7(1)	-7(1)	-5(1)
S(2)	26(1)	21(1)	27(1)	-9(1)	-6(1)	-2(1)

[1] te Velde, G.; Bickelhaupt, F. M.; Baerends, E. J.; van Gisbergen, S. J. A.; Fonseca Guerra, C.; Snijders, J. G.; Ziegler, T. Chemistry with ADF. *J. Comput. Chem.* **2001,** *22,* 931-967.

[2] Fonseca Guerra, C.; Snijders, J. G.; te Velde, G.; Baerends, E. J. Towards an order-N DFT method. *Theor. Chem. Acc.* **1998,** *99,* 391.

[3] Baerends, E. J.; Ziegler, T.; Atkins, A. J.; Autschbach, J.; Bashford, D.; Baseggio, O.; Bérces, A.; Bickelhaupt, F. M.; Bo, C.; Boerritger, P. M.; Cavallo, L.; Daul, C.; Chong, D. P.; Chulhai, D. V.; Deng, L.; Dickson, R. M.; Dieterich, J. M.; Ellis, D. E.; van Faassen, M.; Ghysels, A.; Giammona, A.; van Gisbergen, S. J. A.; Goez, A.; Götz, A. W.; Gusarov, S.; Harris, F. E.; van den Hoek, P.; Hu, Z.; Jacob, C. R.; Jacobsen, H.; Jensen, L.; Joubert, L.; Kaminski, J. W.; van Kessel, G.; König, C.; Kootstra, F.; Kovalenko, A.; Krykunov, M.; van Lenthe, E.; McCormack, D. A.; Michalak, A.; Mitoraj, M.; Mor- ton, S. M.; Neugebauer, J.; Nicu, V. P.; Noodleman, L.; Osinga, V. P.; Patchkovskii, S.; Pavanello, M.; Peeples, C. A.; Philipsen, P. H. T.; Post, D.; Pye, C. C.; Ramanantoan- ina, H.; Ramos, P.; Ravenek, W.; Rodríguez, J. I.; Ros, P.; Rüger, R.; Schipper, P. R. T.; Schlüns, D.; van Schoot, H.; Schreckenbach, G.; Seldenthuis, J. S.; Seth, M.; Snijders, J. G.; Solà, M.; M., S.; Swart, M.; Swerhone, D.; te Velde, G.; Tognetti, V.; Vernooijs, P.; Versluis, L.; Visscher, L.; Visser, O.; Wang, F.; Wesolowski, T. A.; van Wezenbeek, E. M.; Wiesenekker, G.; Wolff, S. K.; Woo, T. K.; Yakovlev, A. L. "ADF2017, SCM, Theoretical Chemistry, Vrije Universiteit, Amsterdam, The Netherlands, https://www.scm.com", 2017.

[4] van Gisbergen, S. J. A.; Snijders, J. G.; Baerends, E. J. Implementation of Time-Dependent Density Functional Response Equations. *Computer Physics Communications* **1999**, *118*, 119-138.

[5] van Lenthe, E.; Baerends, E. J.; Snijders, J. G. Relativistic Regular two-component Hamiltonians. *J. Chem. Phys.* **1993,** *99,* 4597-4610

[6] Lee, C.; Yang, W.; Parr, R. G. Development of the Colle-Salvetti correlation-energy formula into a functional of the electron density. *Phys. Rev. B* **1988,** *37,* 785–789.

[7] Becke, A. D. Density functional thermochemistry. III. The role of exact exchange. *J. Chem. Phys.* **1993,** *98,* 5648–5652.

[8] Ernzerhof, M.; Scuseria, G. E. Assessment of the Perdew-Burke-Ernzerhof. *J. Chem. Phys.* **1999,** *110,* 5029–5036.

[9] Adamo, C.; Barone, V. Toward reliable density functional methods without adjustable parameters: The PBE0 model. *J. Chem. Phys.* **1999,** *110,* 6158-6170.

[10] Yanai, T.; Handy, N. A New Hybrid Exchange-Correlation Functional Using the Coulomb-Attenuating Method. *Chem. Phys. Lett.* **2004**, *393*, 51-57.

[11] van Lenthe, E.; Baerends, E. J. Optimized Slater-type basis sets for the elements 1 – 118. *J. Comput. Chem.* **2003,** *24,* 1142-1156.

[12] Autschbach, J.; Ziegler, T. Calculating Molecular Electric and Magnetic Properties From Time-Dependent Density Functional Perturbation Theory, *J. Chem. Phys.* **2002**, *116*, 891-896.

[13] Autschbach, J.; Ziegler, T.; Patchkovskii, S.; van Gisbergen, S. J. A.; Barends, E. J. Chiroptical Properties from Time-Dependent Functional Theory. II. Optical Rotations of Smal to Medium Sized Organic Molecules. *J. Chem. Phys.* **2002**, *117*, 581-592.

[14] Pye. C. C.; Ziegler, T. An Implementation of the Conductor-Like Screening Model of Solvation within the Amsterdam Density Functional Package. *Theor. Chem. Acc.* **1999**, *101*, 3960-408.

[15] Autschbach, J.; Ziegler, T.; van Gisbergen, S. J. A.; Barends, E. J. Chiroptical Properties from Time-Dependent Density Functional Theory. I. Circular Dischroism Spectra of Organic Molecules. *J. Chem. Phys.* **2002**, *116*, 6930-6940.

[16] Martin, R. L. Natural Transition Orbitals. *J. Chem. Phys.* ***2003****, 118*, 4775-4777.

[17] Aquilante, F.; Autschbach, J.; Carlson, R. K.; Chibotaru, L. F.; Delcey, M. G.; Vico, L. D.; Fdez. Galván, I.; Ferré, N.; Frutos, L. M.; Gagliardi, L.; Garavelli, M.; Giussani, A.; Hoyer, C. E.; Manni, G. L.; Lischka, H.; Ma, D.; Malmqvist, P.-Å.; Müller, T.; Nenov, A.; Olivucci, M.; Pedersen, T. B.; Peng, D.; Plasser, F.; Pritchard, B.; Reiher, M.; Rivalta, I.; Schapiro, I.; Segarra-Martí, J.; Stenrup, M.; Truhlar, D. G.; Ungur, L.; Valentini, A.; Vancoillie, S.; Veryazov, V.; Vysotskiy, V. P.; Weingart, O.; Zapata, F.; Lindh, R. *J. Comput. Chem.* **2016,** *37,* 506–541.

[18] Roos, B. O.; Taylor, P. R.; Siegbahn, P. E. M. A Complete Active Space SCF Method (CASSCF) using a Density Matrix Formulated Super-CIAapproach. *Chem. Phys.* **1980,** *48,* 157–173.

[19] Andersson, K.; Malmqvist, P.-Å.; Roos, B. O.; Sadlev, A. J.; Wolinski, K. Second-Order

Perturbation Theory with a CASSCF Reference Function. *J. Phys. Chem.* **1990,** *94,* 5483–5488.

[20] Douglas, M.; Kroll, N. M. Quantum Electrodynamical Corrections to the Fine Structure of Helium. *Ann. Phys.* **1974,** *82,* 89-155.

[21] Hess, B. A. Applicability of the no-pair equation with free-particle projection operators to atomic and molecular structure calculations. *Phys. Rev. A* **1985,** *32,* 756-763.

[22] Hess, B. A. Relativistic electronic-structure calculations employing a two-component no-pair formalism with external-field projection operators. *Phys. Rev. A* **1986,** *33,* 3742-3748.

[23] Wolf, A.; Reiher, M.; Hess, B. A. The generalized Douglas-Kroll transformation. *J. Chem. Phys.* **2002**, *117,* 9215-9226.

[24] Widmark, P.-O.; Malmqvist, P.-Å.; Roos, B. O. Density-matrix averaged atomic natural orbital (ANO) basis-sets for correlated molecular wave-functions. I. First row atoms. *Theor. Chim. Acta* **1990**, *77,* 291–306.

[25] Roos, B. O.; Lindh, R.; Malmqvist, P.-Å.; Veryazov, V.; Widmark, P.-O. Main group atoms and dimers studied with a new relativistic ANO basis set. *J. Phys. Chem. A* **2004**, *108,* 2851–2858.

[26] Roos, B. O.; Lindh, R.; Malmqvist, P.-Å.; Veryazov, V.; Widmark, P.-O. New relativistic ANO basis sets for transition metal atoms. *J. Phys. Chem. A* **2005**, *109,* 6575.

[27] Gendron, F.; Páez-Hernández, D.; Notter, F.-P.; Pritchard, B.; Bolvin, H.; Autschbach, J. Magnetic properties and electronic structure of neptunyl(VI) complexes: Wavefunctions, orbitals, and crystal-field models. *Chem. Eur. J.* **2014**, *20,* 7994–8011.

[28] Gendron, F.; Pritchard, B.; Bolvin, H.; Autschbach, J. Single-Ion 4f Element Magnetism: an Ab-Initio Look at $Ln(COT)_2^-$.*Dalton Trans.* **2015**, *44,* 19886– 19900.

[29] Autschbach, J. Orbitals for Analyzing Bonding and Magnetism of Heavy-Metal Complexes. *Comments Inorg. Chem.* **2016**, *36,* 215–244.

[30] Malmqvist, P.-A.; Roos, B. O.; Schimmelpfennig, B. The restricted active space (RAS) state interaction approach with spin-orbit coupling. *Chem. Phys. Lett.* **2002**, *357,* 230-240.